ISSN 0252-1075
Research Report No. RR-093

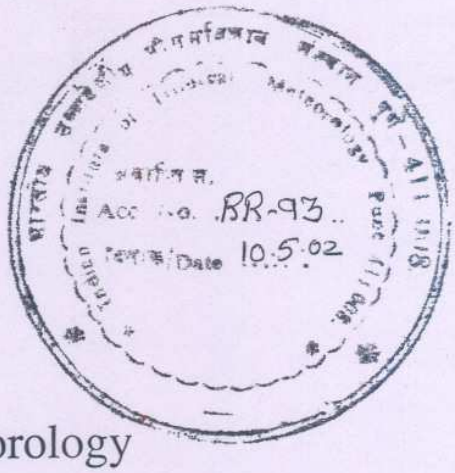

Contribution from
Indian Institute of Tropical Meteorology

PROSPECTS OF PREDICTION OF INDIAN SUMMER MONSOON RAINFALL USING GLOBAL SST ANOMALIES

by

SAHAI A. K., GRIMM A.M., SATYAN V.
and
PANT G. B.

PUNE – 411 008
INDIA

APRIL 2002

Contents

Prospects of Prediction of Indian Summer Monsoon Rainfall using global SST anomalies

A. K. Sahai[1], Alice M. Grimm[2], V. Satyan and G. B. Pant

Indian Institute of Tropical Meteorology, Pune 411 008, India.

ABSTRACT

A methodology is presented for making optimal use of global sea surface temperatures (SST) for long lead prediction of Indian summer monsoon rainfall (ISMR). First, a correlation analysis is used to identify the regions and seasonal lags for which SST is highly correlated with ISMR. Using the first 9 Principal Components (PCs) of SST from these regions it is shown that the historical relationship between ISMR and SST is consistent in recent years. As second step, a strategy for selecting the best 18 predictors (hot spots of the global oceans) is investigated. Using them, the relative roles of different ocean basins in intrannual and decadal variability of ISMR is discussed. It is found that, since mid seventies, South Pacific and North Atlantic SSTs have a dominating influence on ISMR while the influence of east Pacific SSTs has been weakening. It is shown that when the relationship between ISMR and SST in one ocean weakens, the connection with another ocean strengthens. These changes seem to be a part of natural oscillations in the climate system. Therefore, despite the weakening of El Nino Southern Oscillation- ISMR relationship in recent years, most of the variability of ISMR can still be attributed to SST. In the third step, an experimental prediction of ISMR is done based on the first 2 PCs of the SST in the 18 hot spots over the global oceans. The predicted values explain about 80% of the observed variance of ISMR in the model verification period. Finally, a predictive scheme, that is stable and useful in a changing background climate, is discussed and it is shown that a skillful long lead forecasting of ISMR is possible.

---

[1]Currently visiting: Lab. de Meteorologia-Dept.de Fisica, Universidade Federal do Parana, Curitiba-PR, Brazil.

[2]Lab. de Meteorologia-Dept.de Fisica, Universidade Federal do Parana, Curitiba-PR, Brazil.

1. Introduction

The Indian summer monsoon is the major component of Asian summer monsoon. India receives about 80% of the total annual rainfall during summer monsoon season, from June to September. Indian agriculture is largely controlled by rainfall in this season. Small variations in the monsoon onset, in the spatio temporal variability during the season and in the seasonal mean rainfall have the potential for significant economic and social consequences. Therefore, forecasting of all India Summer Monsoon Rainfall (ISMR) is beneficial for more than a billion people and has profound influence on agricultural planning and economic strategies of the country (Swaminathan 1998).

Forecasting of any climatic event requires the knowledge of its spatial and temporal variability. The yearly phenomenon of the monsoon occurs as a spectacular change in convective activity, especially between India and Australia. The Indian Ocean monsoon winds blow from the southwest during summer (wet) and from the northeast in winter (dry). This annual cycle of monsoon exhibits variability on time scales ranging from intraseasonal to decadal (Webster et al. 1998), as happens in most monsoon regions of the globe. It is well known that, even during a particular monsoon season, large scale spatial and intraseasonal variability of the monsoon rainfall over India is evident (Krishnamurthy and Shukla 2000). On interannual time scales, the ISMR exhibits a fairly distinct bienniality (Mooley and Parthasarathy 1984). On decadal scale, there have been alternating periods extending to 3-4 decades with less and more frequent weak monsoons over India (Kripalani and Kulkarni 1997). A large number of studies have analyzed the influence of intraseasonal, biennial and decadal variations on the interannual variability of ISMR (Webster et al. 1998).

The long range forecasting of ISMR was started more than a century ago (Blanford 1884). Since then, many statistical (Thapaliyal 1981; Shukla and Paolino 1983; Mooley et al. 1986; Bhalme et al. 1986; Shukla and Mooley 1987; Gowariker et al. 1991; Navone and Ceccatto 1994; Goswami and Srividya 1996; Sahai et al. 2000) and also dynamical (Manabe et al. 1974; Hann and Manabe 1975; Palmer et al. 1992; Chen and Yen 1994; Ju and Slingo 1995; Sperber and Palmer 1997; Soman and Slingo 1997; Harrison et al. 1997) forecasting models have been developed and used. The principal scientific basis of these models or any seasonal climate forecasting model is founded on the premise that, in tropics, the lower-boundary forcings (SST, sea-ice cover, land-surface temperature and albedo, vegetation cover and type, soil moisture and snow cover etc.), which evolve on a slower time-scale than that of the weather systems themselves, can give rise to significant predictability of statistical characteristics of large scale atmospheric events (Charney and Shukla 1981). Empirical forecasting of ISMR has been performed using combinations of climatic parameters including atmospheric pressure, wind, snow cover, SST, and the phase of ENSO. Though the performance of a few statistical models is found to be better than that of dynamical ones, successful long-range prediction still remains elusive (Webster et al. 1998; Krishna Kumar et al. 1995). The performance of even the most successful acclaimed model of 16 parameters (Gowariker et al. 1991) is not better than the climatological forecast in recent years (Kulkarni 2000; DelSole and Shukla 2001). The secular variation in parameters used as predictors in statistical models is identified as the main problem (Ramage 1983; Krishna Kumar et al. 1995; Sahai et al. 2000). The classical relation between ENSO and ISMR, which has been observed, is that in the majority of years during the ENSO warm (cold) events the ISMR was below (above) normal. Almost all the statistical seasonal prediction schemes of ISMR rely heavily on the change in magnitude of

various ENSO indices from winter (December to February) to spring (March to May) prior to the start of monsoon season. The above average ISMR in 1997, during the greatest El Nino year of the last century, and excess during the moderate El Nino year of 1994 have prompted many studies to reexamine ENSO-ISMR relationship. It has been shown that this relationship is weakening (Kripalani and Kulkarni 1997) and it was proposed (Krishna Kumar et al. 1999) that it might be due to the global warming. It was also observed that this weakening in the relationship is not peculiar to Nino-3 only, but appears to be with any ENSO index. This weakening has been seen not only in recent times, but also in earlier periods , e.g.,1920-1960 (Webster et al. 1998). Notwithstanding, the ISMR time-series is remarkably stable during the last 130 years and the behavior of the decadal variations and the interannual variability in recent years is similar to that in the past (Fig.1). Thus the weakening in relationship cannot be explained by the global warming phenomenon. Therefore, the question arises of the origin of the interannual variability of ISMR in recent years as well as in the past. We propose that it is associated with other oceanic regions also, in addition to the eastern tropical Pacific.

In addition to the SST in the eastern Pacific (Nino-3 region), there are other oceanic regions, such as the warm pool of western Pacific Ocean, the Northwest Pacific Ocean (Ju and Slingo 1995; Soman and Slingo 1997) and the Indian Ocean (Saji et al. 1999) which are identified as linked with the interannual variability of the ISMR. Several studies have documented empirical links between Indian Ocean SST anomalies and monsoon variability. Negative correlations exist between the ISMR and 16 months earlier SST near Indonesia (Nicholls 1983). The links between the ISMR, the Indian Ocean and the tropical eastern Pacific have shown a biennial tendency (Meehl 1987, 1997). Therefore, instead of calculating various indices from tropical Pacific Ocean and using only 6 months lag (December to May) for prediction of the ISMR, it is logical to include all oceans in different seasons with sufficient lag. An attempt in this regard has been made by Clark et al. (2000) who combined various indices from three regions in Indian Ocean and in different seasons to develop a combined index with long lead time, which shows stable relationship throughout the period 1945-1997. We propose to extend this attempt by considering global oceans with sufficient lag.

In a recent paper (Krishnamurthy and Shukla 2000) it is shown that the seasonal mean monsoon rainfall over India consists of an externally forced large-scale (nearly all of India) persistent (nearly the entire season) component and an intraseasonal component that is independent of external forcing. It has been argued that the success in predicting the monsoon rainfall over India will depend on the relative magnitudes of these two components. It has been further pointed out that, if it is possible to establish a predictable relationship between the large scale seasonally persistent component anomalies and the intraseasonal variations, prospects of making more accurate forecasts of the ISMR will certainly improve. In the present communication we propose an approach to achieve this.

Section 2 of this paper deals with the data used in this study and describes the methodology. In section 3, results are presented. In order to assess the prospects for prediction of ISMR using SST, first the consistency of the historical relationship between SST and ISMR in recent decades is examined, then the selecting best predictors are selected and the relative roles of various ocean basins is discussed. It is shown that by using 2 PCs of the selected predictors, prediction of ISMR is possible, and finally a prediction scheme is detailed. The last section summarizes the major results and discusses the future impact of this study.

2. Data and Method

2.1. Data

The monthly SST data, used in this study are from the GISST 2.3b (Rayner et al. 1996) for the period January 1871 to May 2001. The ISMR from June to September for the period 1871-2001 are obtained from IITM data set (Parthasarathy et al. 1994). The SST data were originally on 1°×1° resolution. They were averaged over boxes of 10° latitude× 20° longitude whose centers are 5° latitude×10° longitude apart. Thus, there are overlapping regions between two neighbouring boxes. The purpose of this is to achieve a good spatial resolution (5° ×10°) while working with regions of larger extent (10° ×20°).

2.2. Determination of lags

The correlation coefficients (CC) between the ISMR and the seasonal SST anomalies, and also the anomalies in seasonal tendency of the SST were calculated for various ocean basins in the tropics and the northern extra-tropics (25°S to 65°N). Since our main goal is to do forecasting well in advance, the CC were calculated from 2 season lag to 5 years lag from the start of the ISMR season. For instance, to calculate the index for the 1990 ISMR, SST data used were from March 1985 to February 1990. Before calculating the CC, the previous 5 year running mean is subtracted from all the data sets (the ISMR, the seasonal SST and the seasonal tendency of SST) to filter out local linear trend. For instance, the average value for years 1871 to 1875 was subtracted from the value for 1876 and so on. In many regions the anomalies in seasonal tendency of SST were found to be more correlated with ISMR than the seasonal SST anomalies themselves. This may be because the anomalies in the seasonal tendency of SST represent more appropriately the anomalous response of the ocean-atmosphere coupled system to the seasonal march of the solar radiation than the SST anomalies. The relationships of the SST anomalies and SST tendencies with ISMR, depicted through the CC, are found to be significant and coherent up to 5 year lags in different ocean basins. For example, the strong negative correlation along the central and eastern Pacific prior to the start of monsoon season is in fact equally strong with changed sign and shifted southward about two years before (Fig. 2), indicating the possibility of longer lead time prediction. Therefore, considering lags of up to previous 5 years is justified. Since we are more concerned about the prediction in recent years, this analysis was performed from 1881 to 1989 and data from 1990 to 2001 are kept to verify the performance of the proposed method.

2.3. Methods of selecting best predictor set

When there are many predictors, physical relationships with predictant is not well defined and prediction is the central goal, then a few best among them have to be selected based on robust statistical methods. We have adopted the most commonly used screening procedure known as stepwise regression (Wilks 1995). In this procedure one begins with zero predictor and all possible L simple linear regression between the available L predictors and the predictant are computed. The predictor whose linear relationship is the best among all candidate predictors

is chosen as first predictor. Different ways are proposed to detect the best relationship. One way is to select the predictor with minimum root mean square error ($RMSE$) on the model development set. DelSole and Shukla (2001) have suggested a cross validation scheme for doing this. In this scheme (Michaelsen 1987), model development data is divided into two mutually exclusive sets, independent and dependent. The regression model is developed on each dependent set and prediction is done in corresponding independent set. We have divided the data of model development period (from 1881 to 1989) in N (=109) mutually exclusive dependent and independent sets in which each independent set consists of one year and remaning $N-1$ years are in dependent set.

We have adopted this approach and for each predictor variable we got N independent predicted values along with the observed ones. Values of RMSE are calculated for each predictor. Then the best predictor is that for which $RMSE$ is the minimum. After selecting the first predictor, trial regression equation are again constructed using the first selected predictor in combination with the remaining $L-1$ predictors, and using the above criteria the 2nd predictor is selected. Subsequent steps follow this pattern. The selection procedure is terminated when there is no further significant reduction in RMSE. But the principle of parsimony (Box et al. 1994) requires that an empirical model should employ the smallest number of predictors for adequate representation. In the context of model selection, this principle states that even if a model has less prediction error than another with fewer predictors it should nevertheless be rejected in favor of the model with fewer predictors, if it fails a goodness of fit test. DelSole and Shukla (2001) have discussed many goodness of fit test criteria and we will adopt one, based on Mallow's C_p:

$$C_p = \frac{< e_A^2 >}{(\frac{<e_B^2>}{N-M-P-1})} - (N - 2(P+1)) \tag{1}$$

where A is the reduced model with P predictors, B is the full model with $P+M$ predictors and $< e_A^2 >$ and $< e_B^2 >$ represent the mean squared error of model A and B, respectively. The correct model size can be determined by plotting C_p against $P+1$ (for details see DelSole and Shukla (2001)).

2.4. Measures of predictive skills

In addition to statistics for performance evaluation, viz., CC, root meen square error ($RMSE$), absolute error (AE), we have also calculated one more parameter, which we call performance parameter (PP):

$$PP = 1 - (RMSE/SD)^2 \tag{2}$$

where SD is the standard deviation of the ISMR. PP is same as the skill score defined in Wilks (1995) when the reference forecast is climatology. When $PP > 0$ ($PP < 0$), the forecast will be better (worse) than the climatological forecast (always mean value). If it is close to 1, the forecast will be the best.

3. Results and Discussion

3.1. Predictive relationship between ISMR and global SST

3.1.1. Identifying predictors and assessing SST-ISMR relationship

To begin with, 142 regions of 10° latitude × 20° longitude were identified as having their SST best correlated with ISMR in different season lags. The seasonal SST anomalies or seasonal tendencies of SST in these regions are correlated with ISMR at ≥99.5% significance level. This set of 142 regions (the details are given in Table 1) can be seen as a set of predictors for the ISMR. As there can be overlap between these regions, and there can be the same lag for significant correlation with SST and SST tendencies, the number of independent variables will be much less. We performed an empirical orthogonal function (EOF) analysis to generate independent variables from this set. Data from only 109 years (from 1881 to 1989) were used for EOF analysis and PCs were calculated up to 2001. The first 9 PCs explain more than 50% of the variance and were retained as independent predictor variables for further calculation. The cross validated prediction is done for the model development period using 9 PCs. In this section, the performance of prediction is evaluated to assess the consistency of SST-ISMR relationship in recent years. 21- year sliding $RMSE$, CC and PP are shown in Fig. 3 for this prediction. The CC between observed and predicted ISMR is always significant at 99% level. Except on 7 occasions, the PP is always greater than 0.0. For 109 years, CC=0.64, $RMSE$=62.9 mm and PP=0.41. Then predition is done in model verification period using a regression equation developed for the whole model development period. The values of predicted and observed ISMR are shown in Fig. 4. For the 12 year of model verification period CC=0.71, $RMSE$=40.16 and PP=0.46.

In recent decade the interannual variability of ISMR is much low (SD is less than 65% of long term SD) (see lower panel of Fig. 1). It is observed (from Fig. 3) that generally low variability of the ISMR is associated with comparatively lower CC and PP, i.e., low predictability. But in recent years, despite the low variability, CC and PP are comparable to historical values. Thus, even though the ENSO-ISMR relationship is weakening, SST can still explain most of the interannual variability. It should be mentioned here that recent years (from 1990 onwards) were purposely not included in the model development, i.e., identification of regions and seasons, calculation of EOF loadings and multiple regression. Therefore, the historical relationship between the SST and the ISMR is still consistent in recent years.

3.1.2. Selecting the best predictors and determining the relative roles of different oceans

We have already mentioned that the number of predictors, L (=142), identified above is very large. Therefore, it is necessary to select a few best predictor variables from them. It is not possible to do screening regression on this large set of predictors by considering all possible set of combinations of predictors, as suggested by DelSole and Shukla (2001), because then we have to solve 2^L regression equations. Therefore, we have adopted stepwise regression discussed earlier. The values of $RMSE$ and CC obtained from successively increasing the

number of predictors are shown in Fig. 5. It is difficult to judge from this figure as to when to stop the selection procedure, because at each step there is some improvement. At this stage we used Mallow's C_p statistic. We have plotted C_p against $P+1$ in Fig. 6. To find the correct size, a sensible strategy is to look for a model with a low C_p value which is below but close to 45° line. If there are several such points, we chose the model with smallest value of C_p. Thus, from Fig. 6, the number of predictors plus one is 19, and therefore the 18 predictor model has the most favorable C_p statistic. This point is marked in Fig. 5 and 6. This number seems to be very high for prediction model (next section), but it is convenient to assess the predictability associated with different ocean basins.

The 18 selected regions (3 from Indian Ocean, 10 from Pacific and 5 from Atlantic) are shown in Fig. 7 and the details are given in Table 2. It is interesting to note that this selection scheme has not selected any predictor from eastern Pacific and north Indian Ocean though there are many from these regions in the set of 142. This aspect will be discussed in the next section.

Regions from each ocean basin were combined together by multiplying their sign of CC with ISMR to form six indices: Indian Ocean Index (IOI), West Pacific Ocean Index (WPI), North Pacific Ocean Index (NPI), South Pacific Ocean Index (SPI), North Atlantic Ocean Index (NAI) and South Atlantic Ocean Index (SAI).

$$IOI = (-I1 - I2 + I3)/3$$

$$WPI = (P4 + P9)/2$$

$$NPI = (-P2 - P5 - P8 + P7)/4$$

$$SPI = (P1 + P3 - P6 + P10)/4$$

$$NAI = (-A2 - A3 - A5)/3$$

$$SAI = (A1 - A4)/2$$

The 121 years CC between ISMR and IOI, WPI, NPI, SPI, NAI, SAI and simultaneous Nino3 indices are 0.40, 0.34, 0.31, 0.52, 0.48, 0.37 and -0.48 respectively. The 21-year running CC with these indices and also for comparison simultaneous CC with Nino3 index is shown in Fig. 8. We can clearly observe from this figure that in recent years South Pacific and North Atlantic are more associated with ISMR. This shift of relationship can be seen in the mid seventies, the time around which recent climate shift has been noted (Trenberth 1990). Thus it can be argued that while simultaneous relationship with the eastern Pacific Ocean and the ISMR is decreasing, it is strengthening with the South Pacific and North Atlantic ocean. If we observe it for the entire period we find that weakening and strengthening of relationship between various ocean basins and ISMR is part of natural climatic oscillations with decadal and longer periods.

Using the time series of SST in selected 18 regions in the given lag, a multiple regression model was developed for each dependent data and prediction on independent data is obtained under cross-validation scheme. The 21- year sliding $RMSE$, CC and PP are shown in Fig. 9 for this prediction. The CC between observed and predicted ISMR is always much more significant than 99% level. Except for the period 1930 to 1950 the PP is always greater than 0.5. For 109 years, CC=0.79, $RMSE$=50.9 mm and PP=0.62. Then predition is done for the model verification period using a regression equation developed for the whole model

development period. The values of predicted and observed ISMR are shown in Fig. 10. For the 12 year of model verification period CC=0.77, $RMSE$=48.6 and PP=0.21. It is worth noting that the data for the model verification period were neither used for identification of the 142 predictors nor for the selection of 18 predictors.

3.1.3. EOF analysis of selected predictors

We have seen in the previous section that when prediction was done using 18 predictors, the model performed very good in the development period while the performance in the independent verification period was not that good. DelSole and Shukla (2001) have shown that, if we could identify the most promising parameters then, two to three predictors are sufficient for forecasting of ISMR. Though 18 predictors in the previous section were selected based on robust statistical methods, this number is still very high. The method of selection has not rectified the problem of multicollinearity (mutual correlations among the predictors), which could be a major drawback for linear regression when it is applied for the prediction of independent future data. Therefore, to minimize the redundancy among the predictors and to reduce the number of parameters and also to see the contribution from different time scales to interannual variability of ISMR, the EOF analysis was performed on the above described 18 selected predictors. As before, data used for EOF analysis were up to 1989 and PCs were calculated up to 2001. We have retained the first 2 PCs (they explain about 11.6% and 11.0% of variance, respectively). It should be pointed out that the use of the first two PCs has nothing to do with an arbitrary truncation of EOFs based on a certain mathematical criterion about the eigenvalues, but is due to the assumption that ISMR can be predicted by two promising predictors that best describe the ISMR evolution. The power spectrum of PC1 is shown in Fig. 11 and that of PC2 in Fig. 12. PC1 has significant periodicities of 11.5 and 2.7 years, PC2 of 9.55, 5.4, 3.6 and 2.1 years respectively. The CC of PC1 and PC2 with ISMR is respectively 0.59 and 0.44. The standardized time series of PC1 and PC2 are shown in Fig. 13 and the spatial signatures obtained by regressing the global SST field in simultaneous JJA season upon PC1 and PC2 are shown in Fig. 14. It can be seen from Fig. 14 that PC1 and PC2 both have dominant signatures in eastern, western and central Pacific, while PC2 has some prominent signatures in north Atlantic and Indian Ocean too. The 120 year CC between JJA Nino3 SST index and PC1 and PC2 is respectively -0.33 and -0.32. Using the time series of PC1 and PC2, multiple regression models were developed for each dependent data sets as discussed in earlier section and prediction on independent data set is obtained. 21- year sliding $RMSE$, CC and PP are shown in Fig. 15 for this prediction. The CC between observed and predicted ISMR is almost always significant at 99% level and PP is always greater than zero. For 109 years, CC=0.71, $RMSE$=57.6 mm and PP=0.51. Then predition is done in model verification period using a regression equation developed for the whole model development period. The values of predicted and observed ISMR are shown in Fig. 16. For the 12 years of model verification period CC=0.89, $RMSE$=28.7 and PP=0.72.

3.2. Prediction of ISMR

3.2.1. Empirical prediction using two predictors

The results of the previous section indicate that a long lead and skillful prediction of ISMR is possible using SST only, and to safeguard against any overfitting, two PCs of the selected 18 predictors can be used as potential predictors. The computation of PCs is done as follows. First seasonal mean and seasonal mean tendencies of SST are calculated for each selected region in the specified lag. Then the time series of each region is standardized with mean and standard deviation for the period 1960-1990. In the next step previous 5 year mean is subtracted from each value so that the resulting time series are from 1881-2001. The EOF analysis is performed on these 18 series using data from 1881-1989 and finally, PCs were calculated up to 2001. The cross validation scheme followed in the previous sections is not adequate for validation of prediction, because while selecting the dependent data set for each independent data set, future values from the time series were also included along with the past values. The true prediction will be when only past values are used for model development and prediction is done in the future. To achieve predictions of future data only, we followed the strategy suggested by DelSole and Shukla (2001). For each 25 year segment of the 121 year record, a regression equation was developed and this equation is used for the prediction of the immediately following (independent) 26^{th} year. For example, a forecast for 1906 is generated strictly from the 1881-1905 record; a forecast for 1907 is generated strictly from the 1882-1906 record; and so on. This forecasting scheme may accomodate the changing relationship in time, i.e. changing background climate. Repeating this procedure for all years, we obtained a time series of 96 years independent future forecast from 1906-2001. The values of constant, coefficients of PC1 and PC2 for prediction of each year are shown in Fig. 17. It can be seen from this figure that the constant term and the coefficients are able to capture the low frequency oscillations of background climate. The predicted and observed ISMR values are shown in Fig.18. For 96 year period CC=0.73, $RMSE$=53.91 mm and PP=0.53. The 21-year sliding $RMSE$, CC and PP are shown in Fig. 19 for this prediction. The CC between the observed and predicted ISMR is almost always significant at 99% level. The forecast is not good in 8 years (Table 3), when the absolute error in the forecast is more than 10%. Among these 8 years, forecasted and observed anomalies are of the same sign in 2 years, and in 2 years predicted and observed anomalies both are normal (within 10% of the long term mean). Thus only four years (1919, 1933, 1943 and 1975) are associated with very bad performance of the model. The forecast is exceptionally improving in recent years since mid seventies. For the last 12 years of the model verification period CC=0.89, $RMSE$=24.5 and PP=0.80. Thus when ISMR is delinking with eastern Pacific SST, it is being associated with other oceanic regions of the globe which results in achieving more skillful forecast.

Next we will explore the possibility of including other oceanic regions which are not included in the 18 selected regions. The most important and not selected regions are from north and central Indian Ocean (Clark et al. 2000) and from central and eastern Pacific. From the central and eastern Pacific, the most used predictor is Nino3 tendency (MAM-DJF). We combined this predictor with PC1 and PC2 and prediction is obtained on sliding 25 year segments as discussed above. The values of CC, $RMSE$ and PP for the whole 96 year prediction period are 0.71, 55.62 mm and 0.50 and those for the last 12 years of verification period are 0.73, 36.62 mm and 0.55, respectively. Thus, in comparison to two PCs only, no improvement in the forecast skill is obtained , instead, there is a decrease in skill. This is

in agreement with DelSole and Shukla (2001) who also noted that though ENSO and ISMR have strong simultaneous relationship, its predictive value is low. The other predictor will be obtained by combining three regions in Indian Ocean in different seasons. These regions are of 4° ×4° extent centered in Arabian Sea (20°N, 66°E), northwest of Australia (16°S, 144°E) and central Indian Ocean (4°N, 86°E) in seasons DJF, DJF and SON prior to the start of the monsoon season, respectively. Since we are considering the whole period, we have not removed the linear trend for the period 1945-1995 as was done in Clark et al. (2000). This combined index is used in combination with PC1 and PC2 and prediction is done. The values of CC, $RMSE$ and PP, obtained for this prediction, for the whole 96 year prediction period are 0.73, 53.99 mm and 0.53 and those for the last 12 year verification period are 0.84, 31.38 mm and 0.67 respectively. In this case also the improvement with comparison to only 2 PCs has not been seen.

We are not claiming that there are not hot spots of global ocean other than the 18 selected above. There may be regions which are highly influencing ISMR, but if there are, either they will be highly correlated with some of the selected regions or their influence will be short lived. Thus we can say that, as far as longer term variability and predictability is concerned, PC1 and PC2 contain the optimum information which can be obtained from the SST field three months prior to the start of the monsoon season.

The forecast of ISMR for the year 2002 obtained from the above method is 89.5% of the long term mean.

3.2.2. ISMR Preferred SST for dynamical prediction

It is a matter of long debate that what is the percentage contribution of internal dynamics and that of external forcing in determining the interannual variability of the ISMR. The internal dynamics generates the intraseasonal oscillations and external forcings determine the seasonal mean anomalies on a regional scale of country as a whole. Both together interact to give the temporal and spacial variation of the ISMR. In a recent paper (Krishnamurthy and Shukla 2000) it has been remarked that for making more accurate forecasts of the ISMR, it is necessary to establish a predictable relationship between the large scale seasonally persistent anomalies and intraseasonal variations. This can be achieved as follows. Once the ISMR anomaly is detemined three months in advance, this can be used to generate SST anomalies during the JJA season. This can be done by predicting SST using the first two PCs of the selected 18 regions. At each grid point a multiple regression equation is obtained using the previous 25 years JJA SST and the prediction is done for one year in future. These predicted SST anomalies will be called as the ISMR preferred SST anomaly. These ISMR preferred anomalies for 1991, 1994 and 1997 along with the observed ones are shown in Fig. 20- 22. It can be seen that ISMR preferred SST anomalies are showing the patterns that would produce below normal ISMR in 1991, above normal in 1994 and normal in 1997 as was observed. Commenting on the performance of seasonal forecasting by statistical and dynamical models, Carson (1998) has pointed that the results obtained from the statistical methods are very encouraging and remain a target to be achieved by the dynamical models. He further pointed that it is likely that the best forecast will be produced by an objective combination of both methods. We propose that this objective combination can be achieved when ISMR preferred SST anomalies are used as a boundary condition in an atmospheric general circulation model.

Then it will be possible to predict the spatial and temporal evolution of summer monsoon rainfall over India. This study will be carried out in our future work.

4. Summary and Conclusions

Relationship between the SST and the ISMR for the prediction of the later has been examined in a new perspective. This paper focusses on three issues- (i) changing SST-ISMR relationship, (ii) prediction of the ISMR using SST only and (iii) prediction of the intraseasonal variations using predicted seasonal mean anomaly. It is shown that despite the weakening relationship of ENSO-ISMR in recent years, the relationship between the global SST and the ISMR is consistent for more than a century and any small variation in this relationship is a part of natural oscillations. In fact, the relationship was slightly weaker in late 1920s and mid 1950s when the variability of ISMR was lower than normal (Fig. 1). In the recent years, since the ISMR variability has become lower than normal, the relationship with SST should decrease. Instead, it has become stronger. This can be associated with the climate shift in mid seventies.

The long time series of two meteorological variables -SST and ISMR- has been created independently using different statistical approaches. This study shows the robustness and consistency of these data sets. When SST-ISMR relationship weakens in one ocean it strengthens in another. For the first time the dominant role of the South Pacific and north Atlantic Ocean to ISMR variability is established. It is shown that to a large extent the behavior of ensuing summer monsoon rainfall on the country (India) as a whole can be determined three months in advance using SST only. Thus the anomalously strong and weak monsoon seasons are not stochastic summer patterns, but are part of a longer period and broader scale circulation patterns which are the results of the interaction of ocean- atmosphere coupled system in many seasons in the past. In different decades, about 50-85% of variance associated with the ISMR is explained by SST alone and only 15-50% is explained by other boundary forcings and internal dynamics. A new concept of ISMR preferred SST anomaly is introduced and it is also proposed how to predict intraseasonal oscillations, once the seasonal mean is predicted.

The calculation of two PCs for prediction of ISMR involves all the ocean basins with sufficient time lag and may be able to encompass the evolution of various heat sources and sinks of the coupled ocean- atmosphere system from tropics to extra- tropics. Thus it can be thought that these PCs capture (i) the spatial and temporal heterogeneity of interaction of global oceans with monsoon system and (ii) the biennial oscillation of the coupled system modulated by longer term oscillations. That is why it is able to represent so closely the ISMR. This research will provide new hope to dynamical models like coupled general circulation models, which are designed to capture the evolution of ocean- atmosphere system for climate prediction. It may provide new basis for statistical models, which are hindered by secular variation of predictor- predictant relationship and inter- dependency of predictors. It may also provide new platform for the discussion on global warming and ENSO- monsoon relationships and consequent changes in precipitation patterns. It is not possible to establish definitely cause and effect relationship from an empirical analysis like this, but we can say that the coupling and uncoupling of various ocean basins with monsoon system are parts of natural variability process. Therefore, the observed changes in ENSO- monsoon relationships in recent years can be attributed to the decadal and longer term natural climate variability rather than

longer term trends related to anthropogenic- induced global warming climate changes.

The central point of the present paper is that a long lead and skillful linear statistical prediction of ISMR can be made 3 months prior to the start of the monsoon season using SSTs only. This forecast may be further improved by AGCMs using ISMR preferred SST as a boundary condition. Also, there are possibilties to improve the forecast using non-linear statistical methods and including other slowly evolving boundary forcings, pre-monsson upper air circulation features and other atmospheric parameters.

Acknowledgments We gratefully acknowledge Prof. J. Shukla (COLA, USA) for valuable suggestions and constructive comments on the primary draft of this paper. We had fruitful discussions with R. H. Kripalani, R. Krishnan, K. Rupakumar, K. KrishnaKumar and M. Mujumdar, all from IITM, India. Financial support from CNPq, Brazil to one of the author (A. K. S.) as Visiting Researcher Fellowship, is acknowledged. Finally thanks are due to SSA-MTM Group, Department of Atmospheric Sciences, University of California, Los Angeles for SSA-MTM Toolkit used in this study for spectral analysis and to Brian Doty (COLA) for the GrADS graphic software.

5. References

Blanford H. F., 1884: On the connection of the Himalayan snowfall with dry winds and seasons of draughts in India. *Proc. Roy. Soc. London.* **37**, 3-22.

Bhalme, H. N., S. K. Jadhav, D.A. Mooley, and Bh. V Ramana Murty, 1986: Forecasting of monsoon performance over India. *J. Climatol.* **6**, 347-354.

Box, G. E. P., G. M. Jenkins, and G. C. Reinsel, 1994: *Time series analysis*, 3d ed. Prentice Hall, 598 pp.

Carson, D. J., 1998: Seasonal forecasting. *Q. J. R. Meteorol. Soc.* **124**, 1-26.

Charney, J. G., and J. Shukla, 1981: Predictability of monsoons, in *Monsoon Dynamics,* J. Lighthill and R. P. Pearce, Ed.(University Press, 1981), pp. 99-109.

Chen, T. -C., and M. -C.Yen, 1994: Interannual variation of the Indian monsoon simulated by the NCAR Community Climate Model: Effect of the tropical Pacific SST. *J. Clim.* **7**, 1403-1415.

Clark, C. O., J. E. Cole, and P. J. Webster, 2000: Indian Ocean SST and Indian summer rainfall: Predictive relationships and their decadal variability. *J. Clim.* **13**, 2503-2519.

DelSole, T., and J. Shukla 2001: Linear prediction of Indian monsoon rainfall (communicated).

Goswami, P., and Srividya, 1996: A novel neural network design for long-range prediction of rainfall pattern. *Curr. Sci.* **70**, 447-457.

Gowariker, V., V. Thapliyal, S. M. Kulshrestha , G. S. Mandal, N. Sen Roy, and D. R. Sikka , 1991: A power regression model for long-range forecast of southwest monsoon rainfall over India. *Mausam.* **42**, 125-130.

Hahn, D. G., and S. Manabe, 1975: The role of mountains in the south Asian monsoon circulation. *J. Atmos. Sci.* **32**, 1515-1541.

Harrison, M., M. K. Soman, M. Davy, T. Evans, K. Roberson, and S. Ineson, 1997: Dynamical seasonal prediction of the Indian summer monsoon. *Experimental Long-lead Bulletin.* **6**, 29-32.

Ju, J. , and J. M. Slingo, 1995: The Asian summer monsoon and ENSO. *Q. J. Roy. Meteorol. Soc.* **122**, 1133-1168.

Kripalani, R. H., and A. Kulkarni, 1997: Climate impact of El- Nino/ La- Nina on the Indian monsoon: A new perspective. *Weather.* **52**, 39-46.

Krishna Kumar, K., B. Rajagopalan, and M. A. Cane, 1999: On the weakening Relationship Between the Indian Monsoon and ENSO. *Science.* **284**, 2156-2159.

Krishna Kumar, K., M. K. Soman, and K. Rupakumar, 1995: Seasonal forecasting of Indian summer monsoon rainfall: A review. *Weather.* **50**, 449-467.

Krishnamurthy, V., and J. Shukla, 2000: Intraseasonal and Interannual variability of Rainfall over India. *J. Clim.* **13** 4366-4377.

Kulkarni, A., 2000: paper presented at Annual Monsoon Workshop of Indian Meteorol. Soc., Pune Chapter, 20 December, 2000.

Manabe, S., D. G. Hahn, and J. Hollaway, 1974: The seasonal variation of tropical circulation as simulated by a global model of atmosphere. *J. Atmos. Sci.* 32, 43-83.

Meehl, G. A., 1987: The annual cycle and interannual variability in tropical Pacific and Indian Ocean region. *Mon. Wea. Rev.* **115**, 27-50.

Meehl, G. A., 1997: The south Asian monsoon and the tropospheric biennial oscillation. *J. Clim.* **10**, 1921-1943.

Michaelsen, J. 1987: Cross-validation in statistical climate forecast models. *J. Climate Appl. Meteor.* **26**, 1589-1600.

Mooley, D. A., and B. Parthasarathy, 1984: Fluctuations in All- India summer monsoon rainfall during 1871-1978. *Climatic Change* **6** 287-301.

Mooley, D. A., B. Parthasarathy, and G. B. Pant, 1986: Relationship between all- India summer monsoon rainfall and location of ridge at 500-hPa level along 750 E. *J. Climate Appl. Meteor.* **25**, 633-640.

Navone, H. D., and H. A. Ceccatto, 1994: Predicting Indian monsoon rainfall: A neural network approach. *Clim. Dyn.* **10**, 305-312.

Nicholls, N., 1983: Predicting Indian monsoon rainfall from sea- surface temperature in the Indonesia-north Australia area. *Nature.* **306**, 576-577.

Palmer, T. N., C. Brankowic, P. Viterbo, and M. J. Miller, 1992: Modeling interannual variations of summer monsoons. *J. Clim.* **5**, 399-417.

Parthasarathy, B., A. A. Munot, and D. R. Kothawale, 1994: All India monthly and summer rainfall indices. *Theor. Appl. Climatol.* **49**, 219-224. This data set is available at website http://www.tropmet.res.in/data and referred as IITM All India Rainfall Series.

Ramage, C. S., 1983: The teleconnections and the seige of time. *J. Climatol.* **3**, 223-231.

Rayner, N. A., E. B. Horton, D. E. Parker, C. K. Folland, and R. B. Hackett, 1996: Version 2.2 of the Global sea-Ice and Sea Surface Temperature Data Set, 1903-1994. *Climate Research Technical Note #74*, available from Hadley Centre for Climate and Prediction & Research, Meteorological Office, London Rd, Bracknell, Berkshire, RG12 2SY, England.

Sahai, A. K., M. K. Soman, and V. Satyan, 2000: All India summer monsoon rainfall prediction using an artificial neural network. *Clim. Dyn.* **16**, 291-302.

Saji, N. H., B. N. Goswami, P. N. Vinayachandran, and T. Yamagata, 1999: A dipole mode in the tropical Indian Ocean. *Nature.* **401**, 360-363.

Shukla, J., and D. A. Mooley, 1987: Empirical prediction of the summer monsoon rainfall over India. *Mon. Wea. Rev.* **115**, 695-703.

Shukla, J., and D. A. Paolino, 1983: The Southern Oscillation and long-range forecasting of the summer monsoon rainfall over India. *Mon. Wea. Rev.* **111**, 1830-1837.

Sperber, K. R., and T. N. Palmer, 1996: Interannual tropical rainfall variability in general circulation model simulations associated with the Atmospheric Model Intercomparison Project. *J. Clim.* **9**, 2727-2750.

Soman, M. K., and J. Slingo, 1997: Sensitivity of Asian Summer monsoon to aspects of sea surface temperature anomalies in the tropical pacific ocean. *Q. J. Roy. Meteorol. Soc.* **123**, 309-336.

Swaminathan, M. S., 1998: Padma Bhusan Prof. P. Koteswaram First Memorial Lecture-23rd March 1998: Climate and Sustainable Food Security. *Vayu Mandal.* **28**, 3-10.

Thapaliyal, V., 1981: ARIMA model for long- range prediction of monsoon rainfall in Peninsular India. *India Met. Dep. Monograph Climatology.* **No. 12/81.**

Trenberth, K. E., 1990: recent observed interdecadal climate changes in the Northern Hemisphere. *Bull. Amer. Meteorol. soc.* **71**, 988-993.

Webster, P. J., V. O. Magana, T. N. Palmer, J. Shukla, R. A. Thomas, M. Yanai, and T. Yasunari, 1998: Monsoons: Processes, predictability, and prospects for prediction. *J. Geophys. Res.* **13** 14451-14510.

Willks, D. S., 1995: *Statistical Methods in Atmospheric Sciences*, Academic Press, INC., New York, 467 pp.

Table 1. Table showing details of 142 regions.

REGION	Latitude		Longitude		Season Lag	Sign of CC
	Starting	Ending	Starting	Ending		
1	10	20	40	60	JJA(-4)	+
2	10	20	60	80	JJA(-4)	+
3	15	25	60	80	JJA(-4)	+
4	-5	5	310	330	DJF(-2)	+
5	15	25	50	70	JJA(-4)	+
6	10	20	50	70	JJA(-4)	+
7	5	15	40	60	JJA(-4)	+
8	-5	5	320	340	DJF(-2)	+
9	10	20	70	90	JJA(-4)	+
10	-10	0	0	20	JJA(-8)	-
11	30	40	10	30	SON(-19)	-
12	-20	-10	100	120	DJF(-2)	+
13	5	15	50	70	JJA(-4)	+
14	-25	-15	60	80	MAM(-17)	-
15	5	15	80	100	JJA(-4)	+
16	-5	5	0	20	JJA(-8)	-
17	20	30	200	220	JJA(-8)	+
18	10	20	90	110	SON(-3)	+
19	-10	0	320	340	DJF(-2)	+
20	5	15	60	80	JJA(-4)	+
21	5	15	70	90	JJA(-4)	+
22	-10	0	350	370	JJA(-8)	-
23	20	30	330	350	DJF(-10)	-
24	-5	5	350	370	JJA(-8)	-
25	35	45	350	370	SON(-15)	-
26	10	20	40	60	DJF(-2)	+
27	5	15	280	300	SON(-3)	+
28	-15	-5	100	120	DJF(-2)	+
29	25	35	210	230	JJA(-8)	+
30	-20	-10	110	130	DJF(-2)	+
31	-15	-5	0	20	JJA(-8)	-
32	15	25	320	340	DJF(-10)	-
33	5	15	40	60	DJF(-2)	+
34	-25	-15	80	100	DJF(-10)	-
35	-20	-10	80	100	DJF(-10)	-
36	15	25	330	350	DJF(-10)	-
37	20	30	290	310	JJA(-16)	-
38	5	15	90	110	SON(-3)	+

Table 1—Continued

REGION	Latitude		Longitude		Season Lag	Sign of CC
	Starting	Ending	Starting	Ending		
39	0	10	80	100	JJA(-4)	+
40	-5	5	330	350	DJF(-2)	+
41	10	20	90	110	JJA(-4)	+
42	10	20	80	100	JJA(-4)	+
43	15	25	190	210	SON(-7)	+
44	10	20	270	290	SON(-3)	+
45	0	10	140	160	MAM(-21)	-
46	35	45	0	20	SON(-15)	-
47	0	10	310	330	DJF(-2)	+
48	40	50	190	210	SON(-15)	-
49	10	20	310	330	JJA(-4)	+
50	20	30	130	150	DJF(-14)	+
51	5	15	310	330	SON(-3)	+
52	0	10	300	320	DJF(-2)	+
53	25	35	200	220	JJA(-8)	+
54	-10	0	330	350	DJF(-2)	+
55	55	65	0	20	SON(-19)	-
56	25	35	300	320	SON(-3)	+
57	20	30	280	300	JJA(-16)	-
58	15	25	180	200	SON(-7)	+
59	-25	-15	320	340	SON(-3)	+
60	-15	-5	130	150	DJF(-2)	+
61	25	35	310	330	MAM(-13)	+
62	30	40	280	300	JJA(-8)	+
63	-10	0	100	120	JJA(-20)	+
64	-20	-10	130	150	DJF(-2)	+
65	20	30	210	230	JJA(-8)	+
66	15	25	320	340	JJA(-4)	+
67	10	20	280	300	SON(-3)	+
68	0	10	50	70	JJA(-4)	+
69	-20	-10	190	210	JJA(-8)	+
70	40	50	180	200	SON(-15)	-
71	10	20	50	70	DJF(-2)	+
72	-25	-15	100	120	DJF(-2)	+
73	-20	-10	70	90	DJF(-10)	-
74	0	10	320	340	DJF(-2)	+
75	-10	0	30	50	DJF(-2)	+
76	15	25	50	70	DJF(-2)	+

Table 1—Continued

REGION	Latitude		Longitude		Season Lag	Sign of CC
	Starting	Ending	Starting	Ending		
77	-15	-5	160	180	DJF(-2)	+
78	20	30	330	350	JJA(-4)	+
79	0	10	350	370	JJA(-8)	-
80	30	40	0	20	SON(-15)	-
81	0	10	310	330	SON(-3)	+
82	5	15	80	100	SON(-3)	+
83	45	55	310	330	DJF(-14)-SON(-15)	-
84	-25	-15	210	230	JJA(-8)-MAM(-9)	+
85	-25	-15	220	240	JJA(-8)-MAM(-9)	+
86	-25	-15	250	270	JJA(-8)-MAM(-9)	+
87	-25	-15	200	220	JJA(-8)-MAM(-9)	+
88	50	60	310	330	DJF(-14)-SON(-15)	-
89	-25	-15	240	260	JJA(-8)-MAM(-9)	+
90	-25	-15	230	250	JJA(-8)-MAM(-9)	+
91	45	55	300	320	DJF(-14)-SON(-15)	-
92	-20	-10	200	220	JJA(-8)-MAM(-9)	+
93	-25	-15	260	280	JJA(-8)-MAM(-9)	+
94	30	40	120	140	DJF(-14)-SON(-15)	+
95	-15	-5	180	200	SON(-15)-JJA(-16)	+
96	-10	0	320	340	DJF(-2)-SON(-3)	+
97	45	55	320	340	DJF(-14)-SON(-15)	-
98	40	50	180	200	SON(-15)-JJA(-16)	-
99	50	60	300	320	SON(-3)-JJA(-4)	+
100	25	35	190	210	JJA(-8)-MAM(-9)	+
101	-15	-5	170	190	SON(-15)-JJA(-16)	+
102	-20	-10	210	230	JJA(-8)-MAM(-9)	+
103	25	35	200	220	JJA(-8)-MAM(-9)	+
104	0	10	180	200	SON(-15)-JJA(-16)	+
105	40	50	190	210	SON(-15)-JJA(-16)	-
106	40	50	200	220	DJF(-2)-SON(-3)	-
107	25	35	120	140	DJF(-14)-SON(-15)	+
108	50	60	320	340	DJF(-14)-SON(-15)	-
109	-20	-10	110	130	DJF(-2)-SON(-3)	+
110	-20	-10	330	350	JJA(-12)-MAM(-13)	+
111	-20	-10	80	100	JJA(-20)-MAM(-21)	-
112	-5	5	100	120	SON(-3)-JJA(-4)	+
113	35	45	210	230	SON(-11)-JJA(-12)	+
114	-25	-15	270	290	JJA(-8)-MAM(-9)	+

Table 1—Continued

REGION	Latitude		Longitude		Season Lag	Sign of CC
	Starting	Ending	Starting	Ending		
115	15	25	120	140	JJA(-12)-MAM(-13)	-
116	30	40	210	230	SON(-11)-JJA(-12)	+
117	20	30	190	210	MAM(-5)-DJF(-6)	-
118	-25	-15	220	240	JJA(-4)-MAM(-5)	-
119	10	20	150	170	SON(-19)-JJA(-20)	+
120	-10	0	210	230	MAM(-17)-DJF(-18)	+
121	45	55	320	340	SON(-15)-JJA(-16)	+
122	40	50	310	330	DJF(-14)-SON(-15)	-
123	-10	0	220	240	MAM(-17)-DJF(-18)	+
124	-15	-5	330	350	JJA(-12)-MAM(-13)	+
125	-25	-15	60	80	MAM(-17)-DJF(-18)	-
126	0	10	170	190	SON(-15)-JJA(-16)	+
127	25	35	290	310	JJA(-16)-MAM(-17)	-
128	-20	-10	100	120	DJF(-2)-SON(-3)	+
129	40	50	190	210	DJF(-2)-SON(-3)	-
130	55	65	300	320	SON(-7)-JJA(-8)	-
131	-15	-5	130	150	JJA(-4)-MAM(-5)	-
132	50	60	300	320	DJF(-14)-SON(-15)	-
133	-15	-5	330	350	DJF(-2)-SON(-3)	+
134	-15	-5	130	150	DJF(-2)-SON(-3)	+
135	-5	5	180	200	SON(-15)-JJA(-16)	+
136	30	40	200	220	SON(-11)-JJA(-12)	+
137	-15	-5	80	100	JJA(-20)-MAM(-21)	-
138	-25	-15	70	90	JJA(-8)-MAM(-9)	+
139	15	25	280	300	SON(-15)-JJA(-16)	+
140	-10	0	30	50	MAM(-5)-DJF(-6)	+
141	15	25	300	320	SON(-15)-JJA(-16)	+
142	15	25	190	210	MAM(-5)-DJF(-6)	-

Note. — Values in braces () in season lag represent those many seasons prior to ISMR.

Table 2. Table showing details of 18 regions.

REGION	Latitude		Longitude		Season Lag	Sign of CC
	Starting	Ending	Starting	Ending		
I1	-25	-15	60	80	MAM(-17)	-
A1	-5	5	310	330	DJF(-2)	+
A2	30	40	10	30	SON(-19)	-
P1	-20	-10	190	210	JJA(-8)	+
A3	55	65	0	20	SON(-19)	-
A4	-15	-5	0	20	JJA(-8)	-
I2	-20	-10	70	90	DJF(-10)	-
I3	-20	-10	130	150	DJF(-2)	+
P2	40	50	180	200	SON(-15)	-
A5	45	55	310	330	DJF(-14)-SON(-15)	-
P3	-25	-15	240	260	JJA(-8)-MAM(-9)	+
P4	0	10	170	190	SON(-15)-JJA(-16)	+
P5	20	30	190	210	MAM(-5)-DJF(-6)	-
P6	-25	-15	220	240	JJA(-4)-MAM(-5)	-
P7	30	40	210	230	SON(-11)-JJA(-12)	+
P8	40	50	180	200	SON(-15)-JJA(-16)	-
P9	10	20	150	170	SON(-19)-JJA(-20)	+
P10	-10	0	210	230	MAM(-17)-DJF(-18)	+

Note. — Here I1 to I3 denote regions from Indian Ocean, P1 to P10 from Pacific and A1 to A5 from Atlantic. Values in braces () in season lag represent those many seasons prior to ISMR.

Table 3. Table showing predicted and observed ISMR values. The regression coefficients associated with PC1 and PC2 with constant of regression is also shown.

Year	Predicted Anomaly (mm)	Observed Anomaly (mm)	Forecast Error(%)	Regression Coefficients. Constantant	PC1	PC2
1906	94.40	32.75	-7.23	2.68	46.72	33.75
1907*	-2.25	-74.75	-8.50	-.70	42.60	35.36
1908	27.82	44.85	2.00	-3.66	45.63	28.98
1909	12.00	36.85	2.91	-3.51	46.04	29.12
1910	57.55	82.55	2.93	-3.37	46.50	26.69
1911	-120.00	-115.85	0.49	-4.69	47.08	32.01
1912	-5.00	-46.25	-4.84	-4.08	46.94	32.42
1913	-39.19	-68.15	-3.40	-6.96	46.22	33.13
1914	-6.76	45.85	6.17	-11.90	52.96	37.70
1915	-58.57	-71.75	-1.55	-15.88	58.37	37.85
1916	73.85	98.05	2.84	-18.88	58.27	38.45
1917	121.68	151.75	3.53	-18.29	58.58	40.46
1918	-172.67	-201.45	-3.38	-17.92	59.21	40.96
1919**	-105.33	32.05	16.11	-22.46	59.79	41.24
1920	-78.38	-133.45	-6.46	-21.18	59.77	29.22
1921	62.57	13.75	-5.73	-26.02	61.92	34.05
1922	83.52	16.65	-7.84	-29.91	61.48	33.06
1923	-40.63	-29.15	1.35	-31.84	60.96	29.22
1924	-21.76	10.45	3.78	-32.59	59.92	30.14
1925	-60.51	-48.75	1.38	-27.01	55.27	29.51
1926	-11.81	50.35	7.29	-25.65	55.73	30.42
1927	-24.72	0.75	2.99	-22.59	56.76	27.77
1928	-58.67	-84.55	-3.04	-20.26	56.14	28.34
1929	26.61	-31.25	-6.79	-20.44	57.47	28.34
1930	-78.70	-47.95	3.61	-20.20	56.35	25.66
1931	11.63	24.85	1.55	-17.40	54.18	23.72
1932	-26.30	-49.05	-2.67	-14.59	59.52	23.68
1933**	-48.02	123.35	20.10	-14.16	58.51	24.49
1934	37.84	60.95	2.71	-9.47	48.17	34.16
1935	-34.25	-8.95	2.97	-10.36	46.80	36.08
1936*	-23.28	56.05	9.30	-10.16	45.59	35.50
1937	20.21	-10.55	-3.61	-7.20	50.16	32.09
1938	52.10	55.75	0.43	-6.80	48.64	32.44
1939	-75.19	-62.85	1.45	-5.33	48.95	31.33
1940	-26.92	0.85	3.26	-6.62	48.30	30.95
1941	-98.63	-124.15	-2.99	-4.28	45.34	31.47
1942	60.42	105.25	5.26	-6.37	46.28	30.93
1943**	-87.03	15.85	12.07	-7.11	41.23	31.85

Table 3—Continued

Year	Predicted Anomaly (mm)	Observed Anomaly (mm)	Forecast Error(%)	Regression Coefficients Constantant	PC1	PC2
1944	26.34	68.15	4.90	-.67	28.86	22.63
1945	69.04	58.35	-1.25	-2.57	31.87	27.52
1946	-6.92	51.35	6.83	1.31	27.72	24.35
1947	42.55	93.35	5.96	4.94	29.33	24.05
1948	13.77	21.75	0.94	8.90	37.72	27.39
1949	27.15	51.55	2.86	11.09	37.25	28.29
1950	-5.92	24.65	3.59	12.60	37.75	28.59
1951	-83.01	-113.65	-3.59	15.92	35.10	29.23
1952	-30.40	-59.25	-3.38	13.32	36.89	31.59
1953*	-12.17	70.45	9.69	12.97	37.90	32.11
1954	29.22	33.05	0.45	19.22	33.66	33.88
1955	52.50	77.85	2.97	22.80	35.93	34.96
1956	68.56	130.95	7.32	23.73	36.87	35.21
1957*	30.48	-63.95	-11.08	27.62	39.16	38.05
1958	30.82	36.85	0.71	26.90	38.70	38.29
1959	16.54	91.55	8.80	24.05	40.03	33.24
1960*	59.15	-12.65	-8.42	27.09	40.26	32.40
1961*	96.58	167.75	8.35	24.82	38.45	31.03
1962	16.42	-42.65	-6.93	25.77	40.48	37.03
1963	-3.98	5.15	1.07	25.53	42.58	35.51
1964	46.91	70.15	2.73	27.20	43.21	37.10
1965	-105.60	-143.15	-4.40	28.51	43.23	36.38
1966*	-41.00	-112.35	-8.37	28.14	44.48	40.62
1967	62.69	7.55	-6.47	27.40	43.70	41.57
1968*	-11.46	-97.95	-10.15	25.44	42.87	40.94
1969*	79.96	-21.25	-11.87	19.28	47.77	49.09
1970	95.39	87.15	-.97	14.79	46.76	42.68
1971	76.71	34.35	-4.97	17.06	50.96	44.50
1972*	-89.96	-199.65	-12.87	13.37	50.68	42.63
1973*	-8.10	61.05	8.11	8.70	54.44	47.91
1974*	-25.16	-104.45	-9.30	9.53	51.40	51.18
1975**	-9.38	110.15	14.02	3.13	44.90	59.45
1976	-23.49	4.25	3.25	8.44	50.26	53.99
1977	11.56	30.75	2.25	8.73	53.82	54.04
1978*	140.59	56.85	-9.82	9.65	53.14	54.38
1979	-87.44	-144.65	-6.71	2.46	62.08	41.17
1980	81.54	30.25	-6.02	-1.39	70.75	36.77
1981	-47.67	-.55	5.53	-3.33	72.02	31.91

Table 3—Continued

Year	Predicted Anomaly (mm)	Observed Anomaly (mm)	Forecast Error(%)	Regression Coefficients Constantant	PC1	PC2
1982*	-38.31	-117.15	-9.25	-4.42	66.93	31.25
1983	48.82	103.25	6.38	-5.30	63.14	37.23
1984	49.38	-15.85	-7.65	-4.93	67.27	36.08
1985*	-7.58	-92.55	-9.97	-11.54	65.07	35.80
1986	-110.60	-109.35	0.15	-13.16	62.93	39.14
1987	-90.41	-155.25	-7.61	-16.77	58.63	36.04
1988	81.07	108.95	3.27	-18.81	59.53	38.52
1989	-20.88	14.15	4.11	-19.85	61.99	39.65
1990	18.89	56.05	4.36	-21.32	63.56	36.92
1991	-80.18	-67.85	1.45	-21.56	66.60	41.55
1992	-59.27	-67.85	-1.01	-20.74	65.09	41.84
1993	14.66	44.05	3.45	-20.32	66.09	41.86
1994	54.12	85.65	3.70	-17.68	66.50	40.67
1995	-41.30	-62.25	-2.46	-14.69	66.47	45.44
1996	2.41	-.15	-.30	-15.38	67.41	45.10
1997	16.37	18.05	0.20	-14.97	67.62	45.75
1998	33.74	-1.35	-4.12	-12.51	61.99	43.51
1999	-61.58	-32.05	3.46	-17.80	63.55	43.32
2000	-85.42	-62.55	2.68	-12.62	66.34	35.64
2001	-36.23	-62.55	-3.09	-16.54	62.36	37.66

Note. — * is showing when error is greater than 8% but forecasted and observed anomalies either both are normal or both are of same sign. ** is showing very bad prediction.

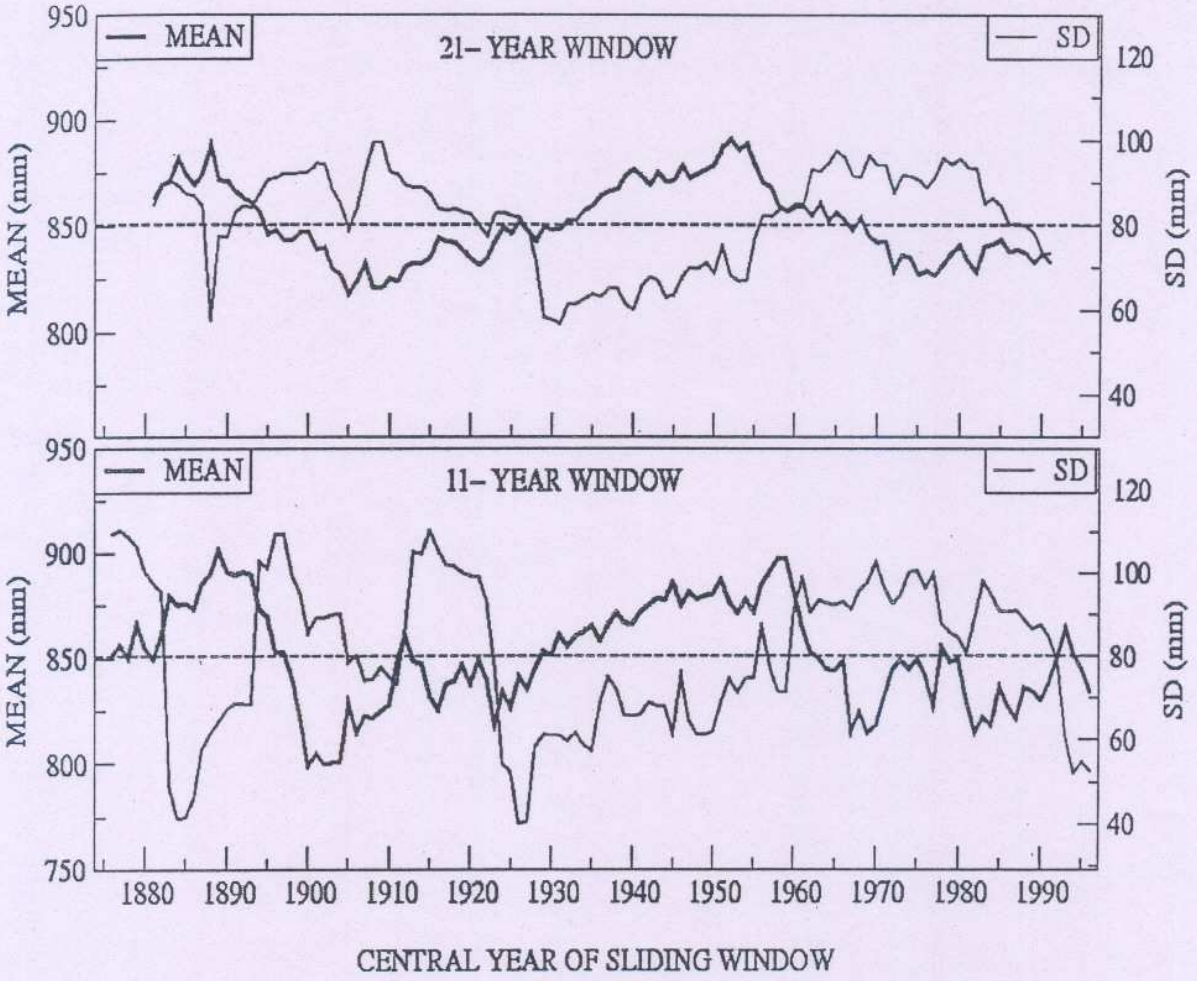

Fig. 1.— The 21-year (upper panel) and 11- year (lower panel) sliding mean and standard deviation of ISMR. In both panels the dotted line represents the long term mean(851.2 mm) and SD (80.0 mm) both.

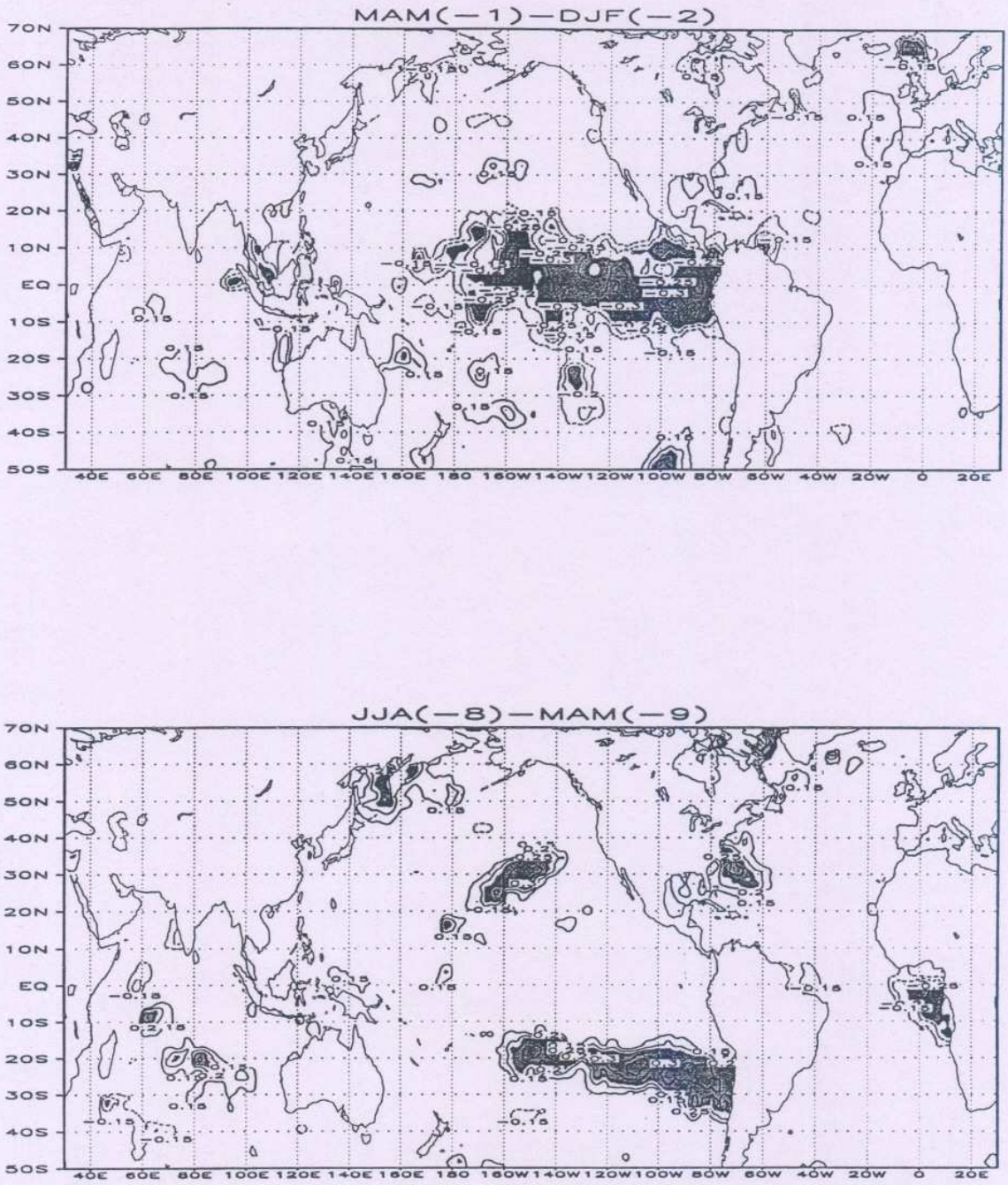

Fig. 2.— Correlation coeficients between ISMR and SST for the period 1881-1989. Contour intervals are 0.05 and the contours of -0.1, -0.05, 0.0, 0.05, 0.1 are dropped. Dotted (continuous) line represents negative (positive) values. The regions where CC is greater than 99% significance level are shaded.

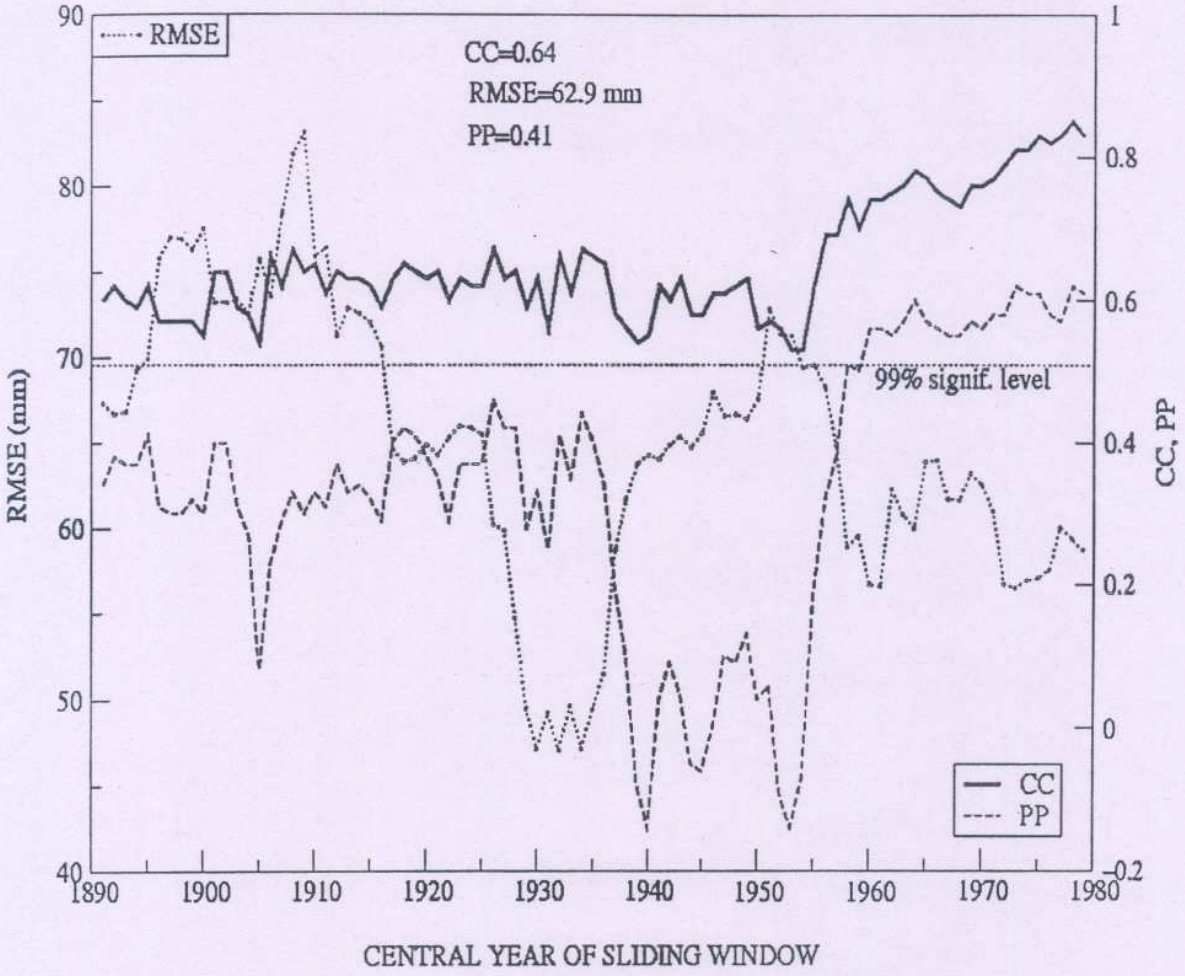

Fig. 3.— The 21- year sliding RMSE , CC and PP are shown for independent data of model development period. In this case prediction is done using 9 PCs calulated from all 142 regions. 99% significance level line for CC is also drawn.

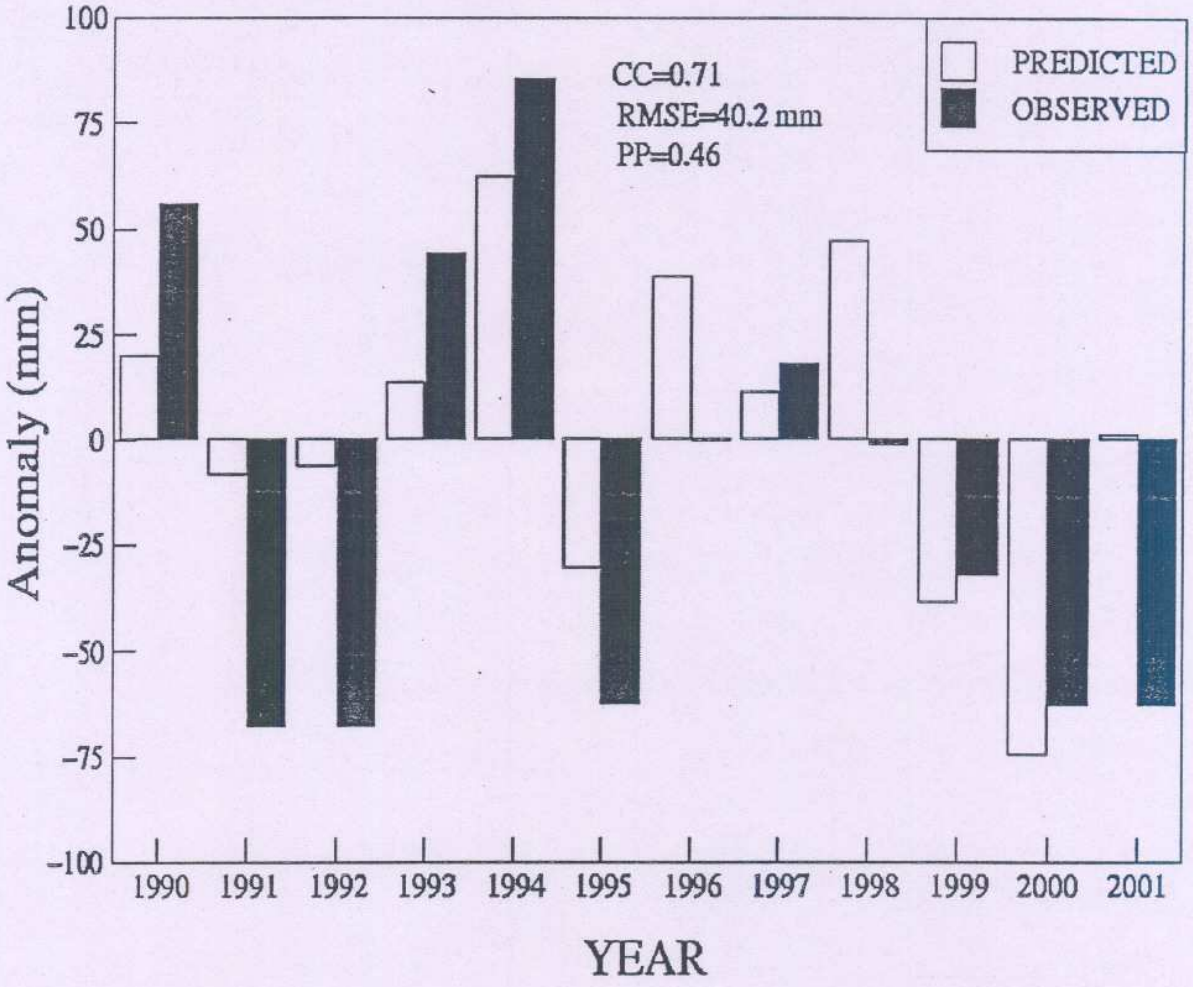

Fig. 4.— Predicted and observed ISMR anomalies for model verification period. The perdiction in this case was done using 9 PCs calulated from all 142 regions. Values of CC, RMSE and PP for this period are also shown.

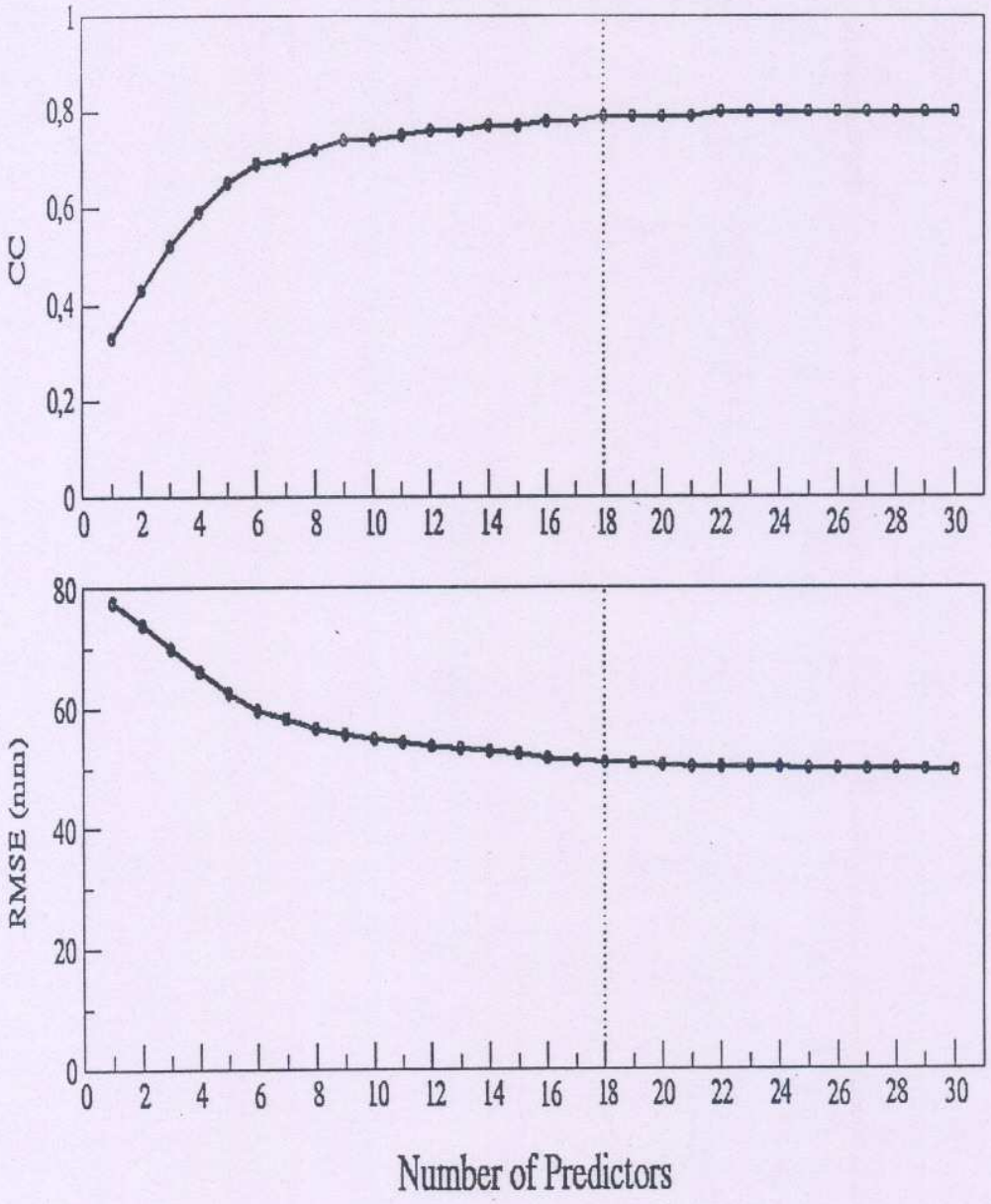

Fig. 5.— The RMSE and CC versus number of predictors for independent data of model development period.

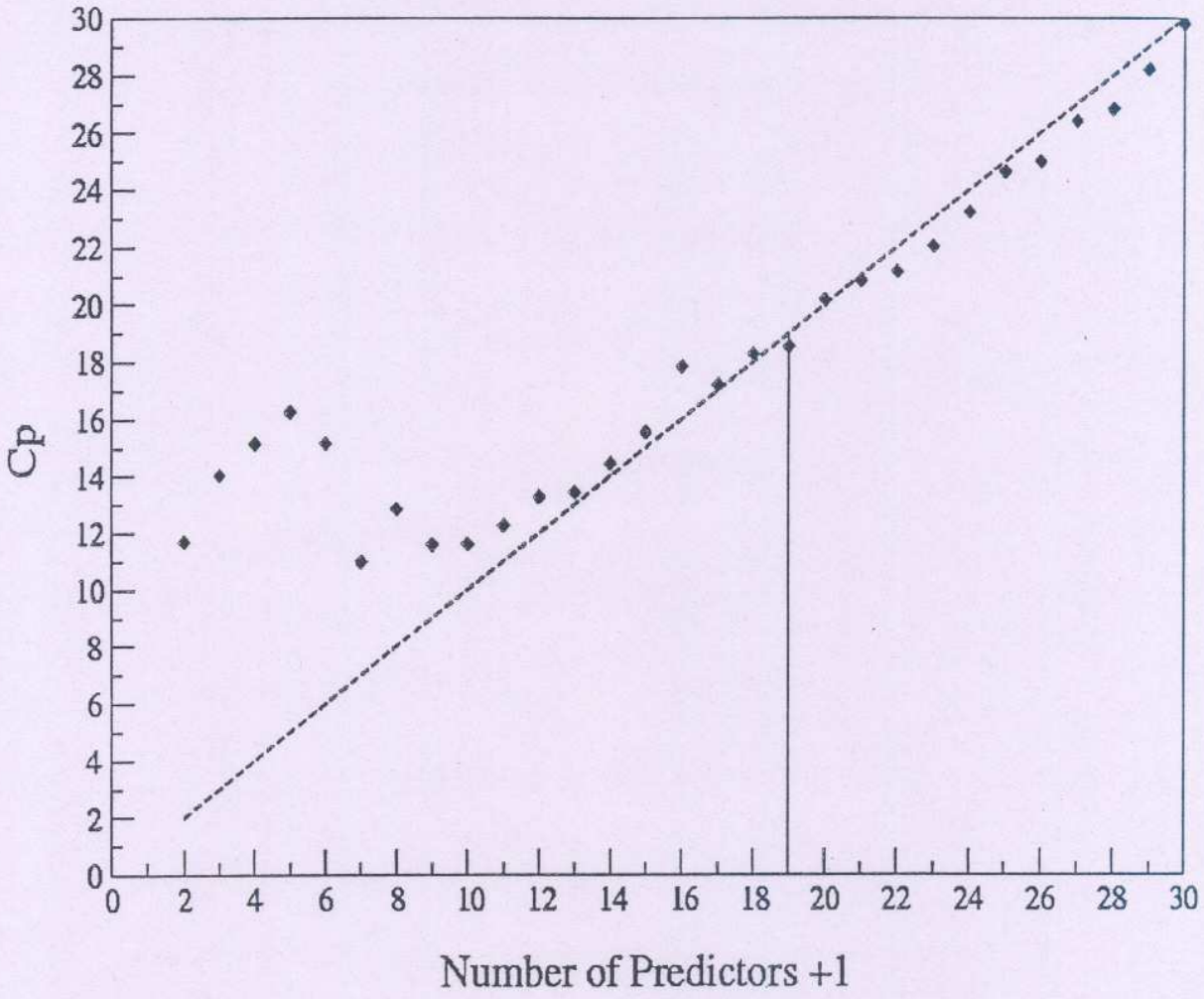

Fig. 6.— Mallow's C_p statistic for selected parameters when screening was done using stepwise regression (Fig. 5). Also shown is 45° line (dash).

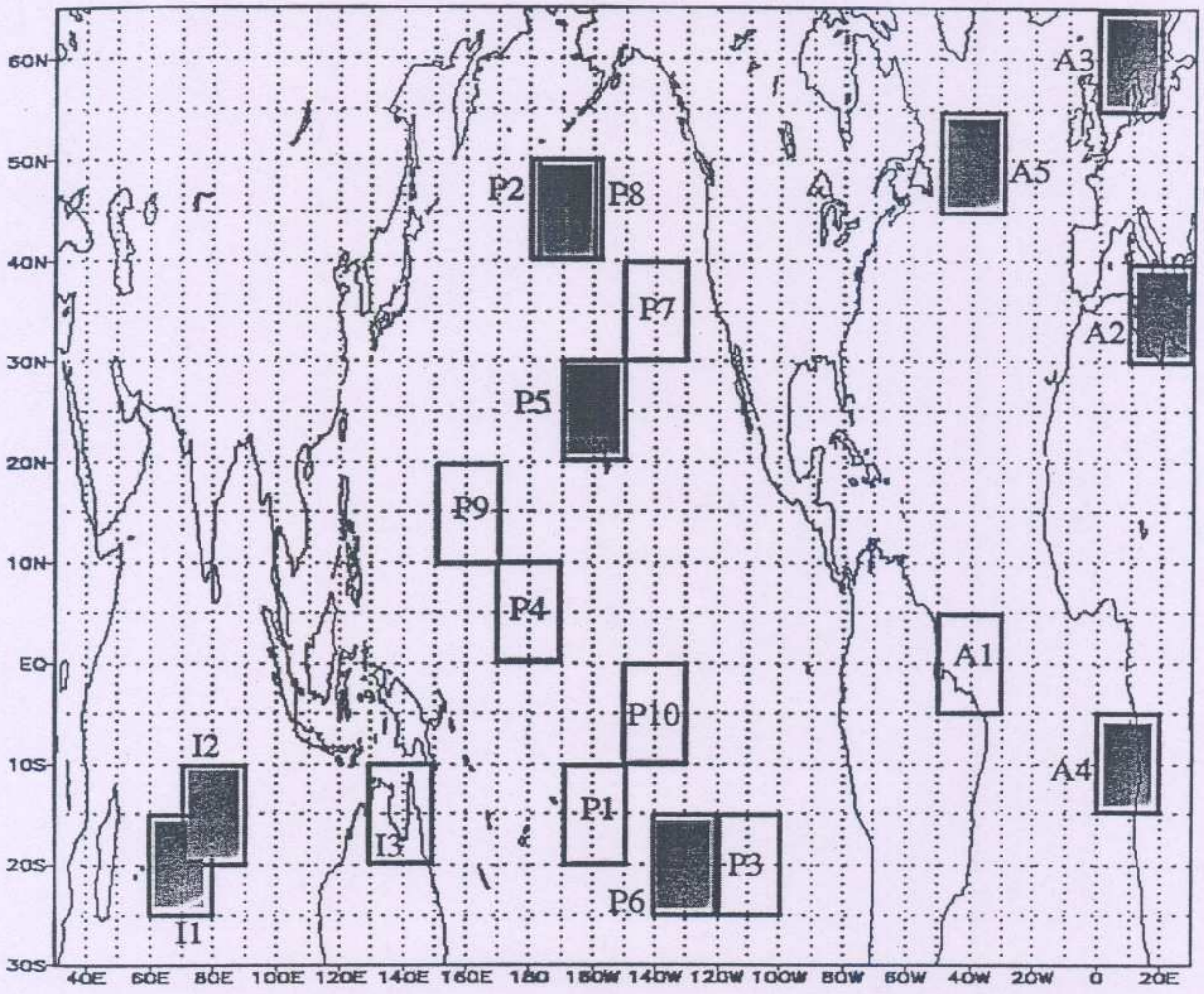

Fig. 7.— Location of 18 selected regions. Regions with negative signs of CC are shaded.

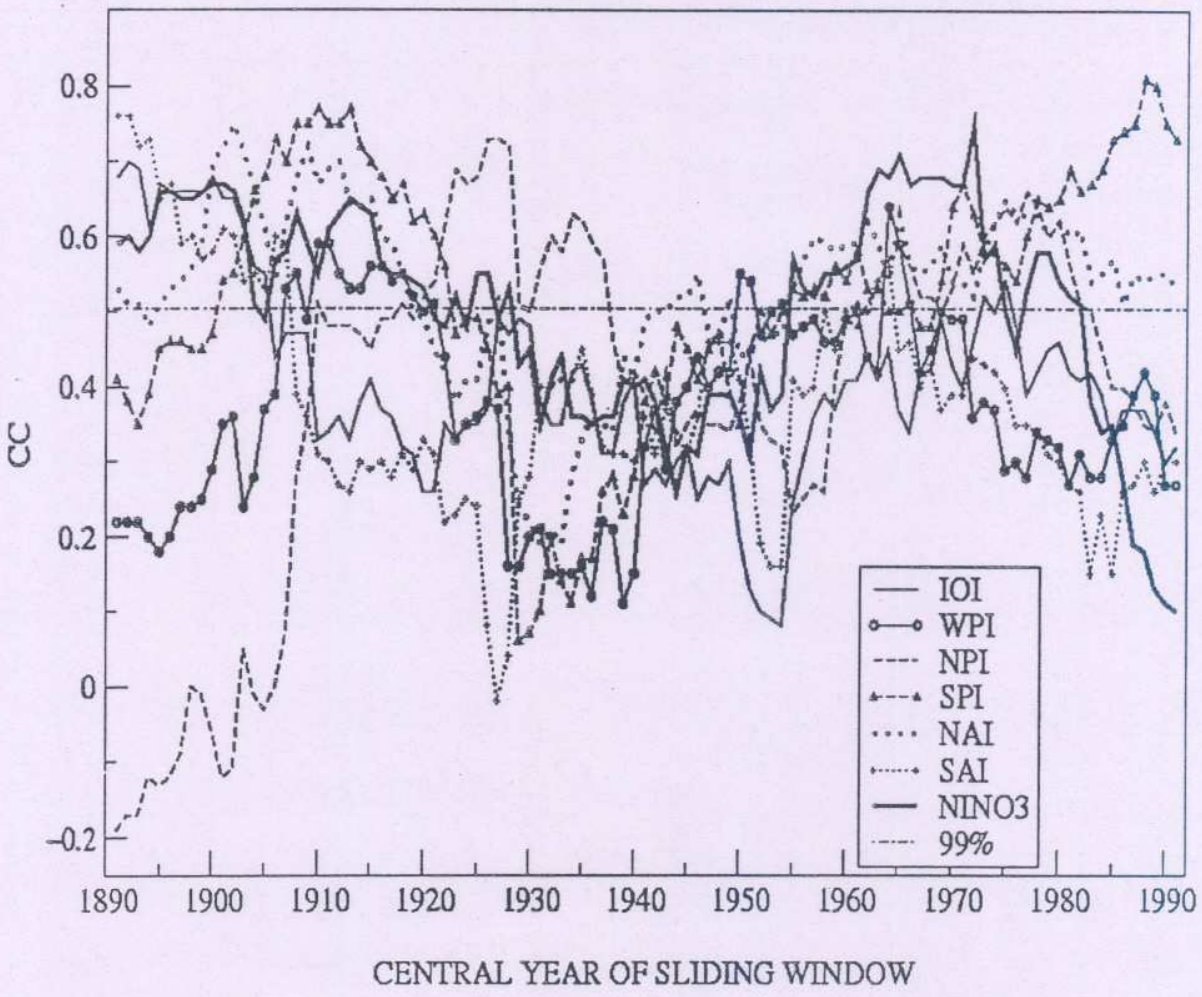

Fig. 8.— The 21- year sliding CC for IOI, WPI, NPI, SPI, NAI, SAI and Nino3 index with ISMR are shown. CC with Nino3 index is simultaneous (JJA SST) and for comparison, values are multiplied by -1. 99% significance level line for CC is also drawn.

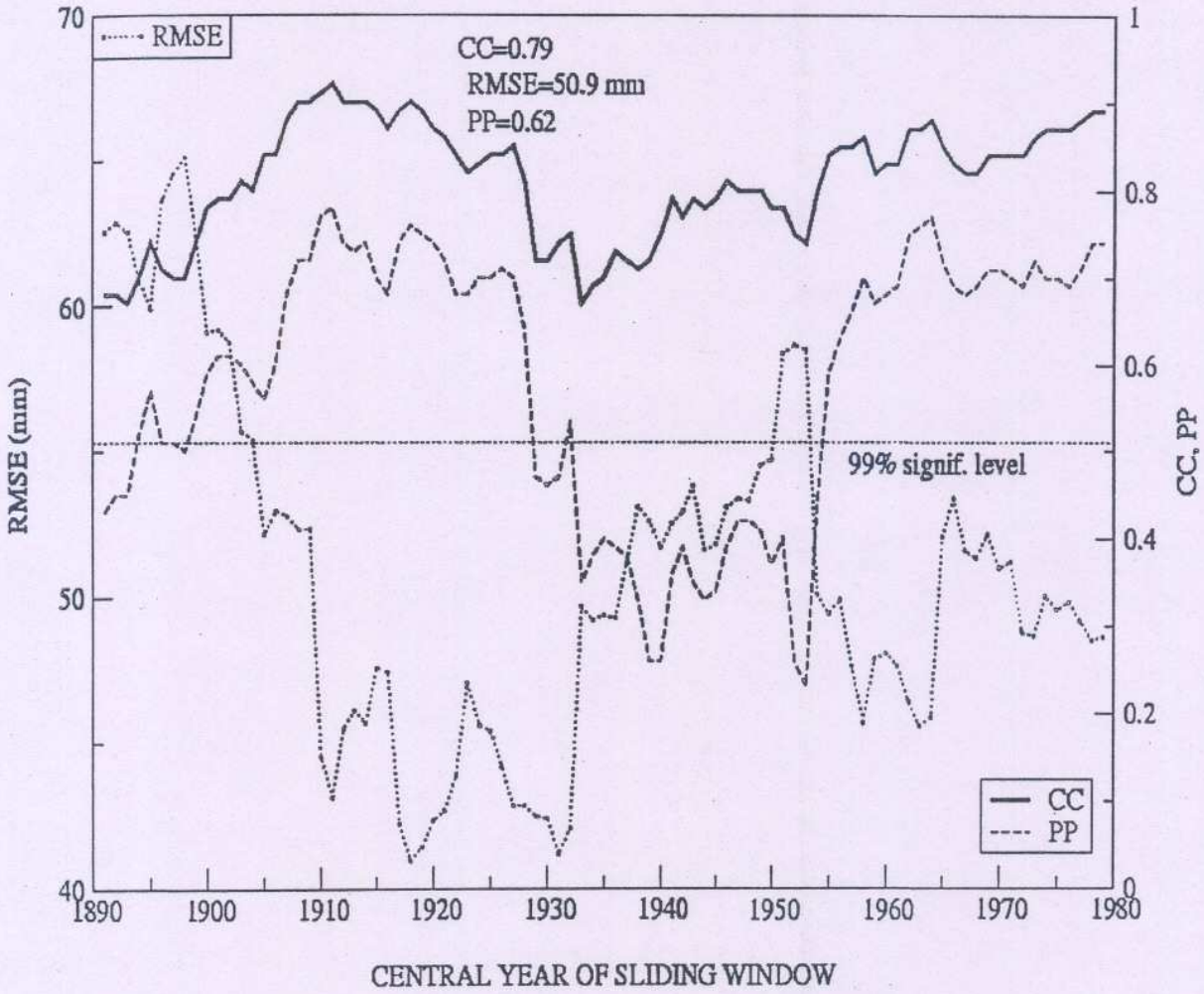

Fig. 9.— The 21- year sliding RMSE , CC and PP are shown for independent data of model development period. In this case prediction is done using 18 selected predictors. 99% significance level line for CC is also drawn.

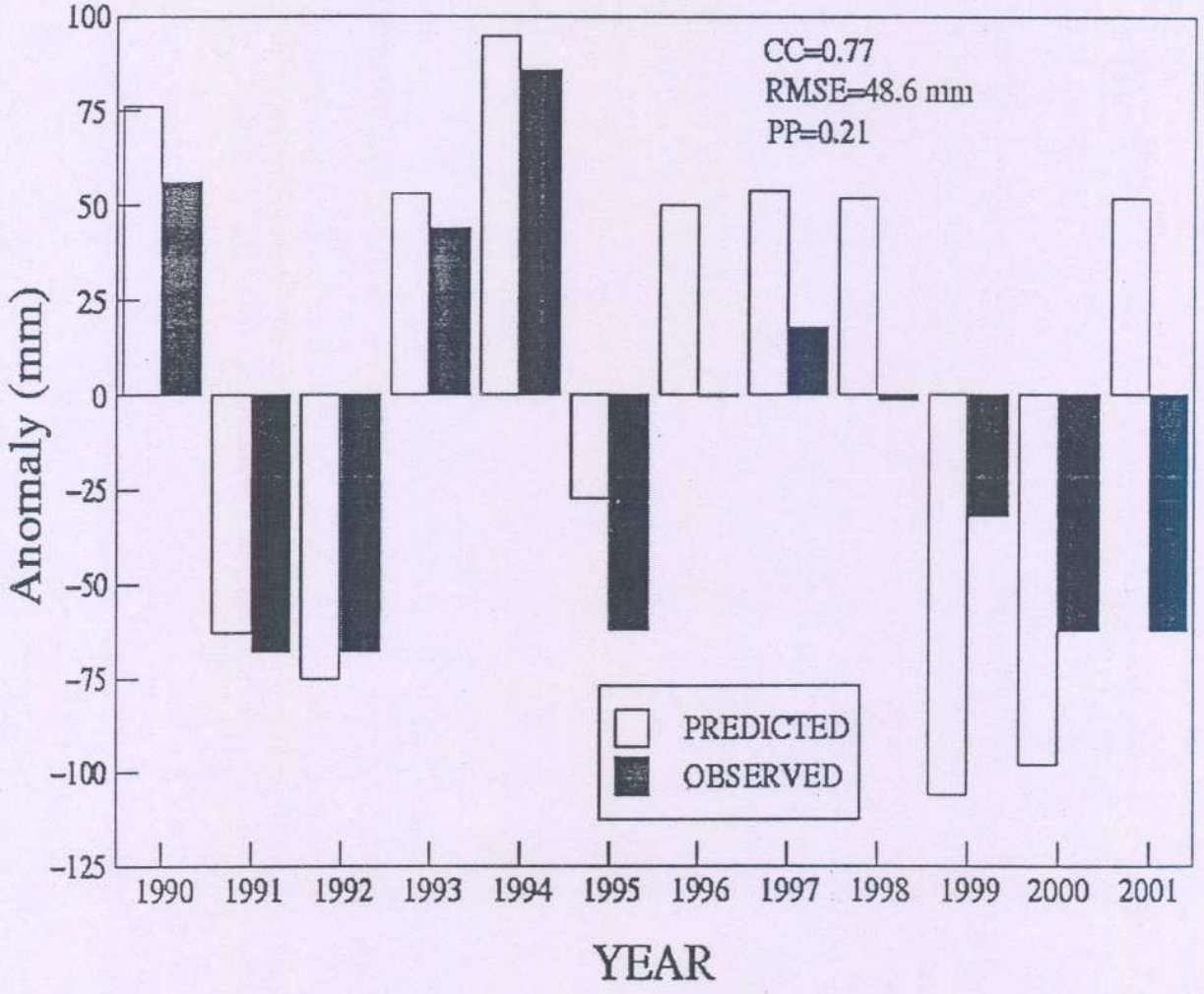

Fig. 10.— Predicted and observed ISMR anomalies for model verification period. The perdiction in this case was done using 18 selected predictors. Values of CC, RMSE and PP for this period are also written.

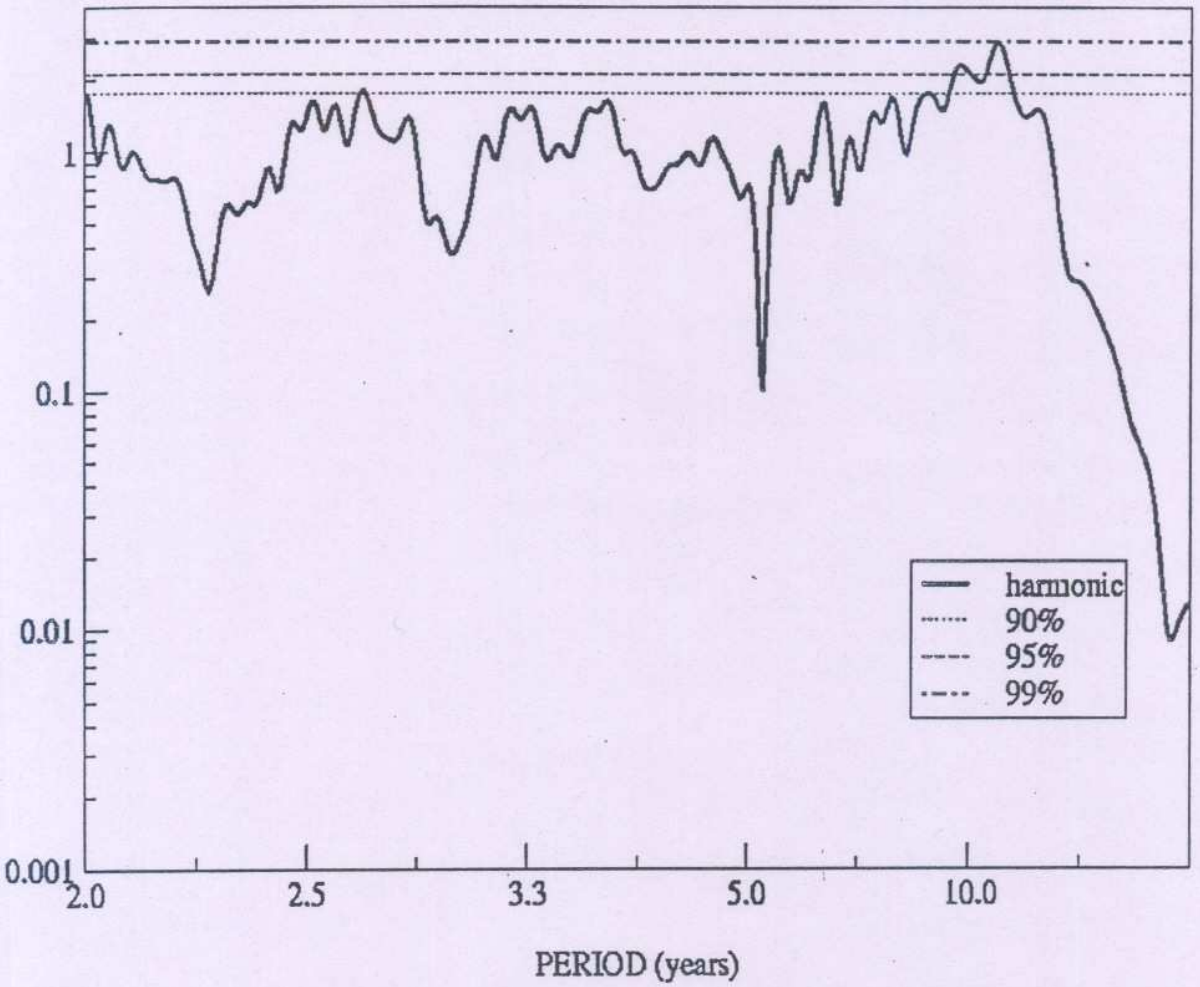

Fig. 11.— Power spectrum of time series of PC1 is shown.

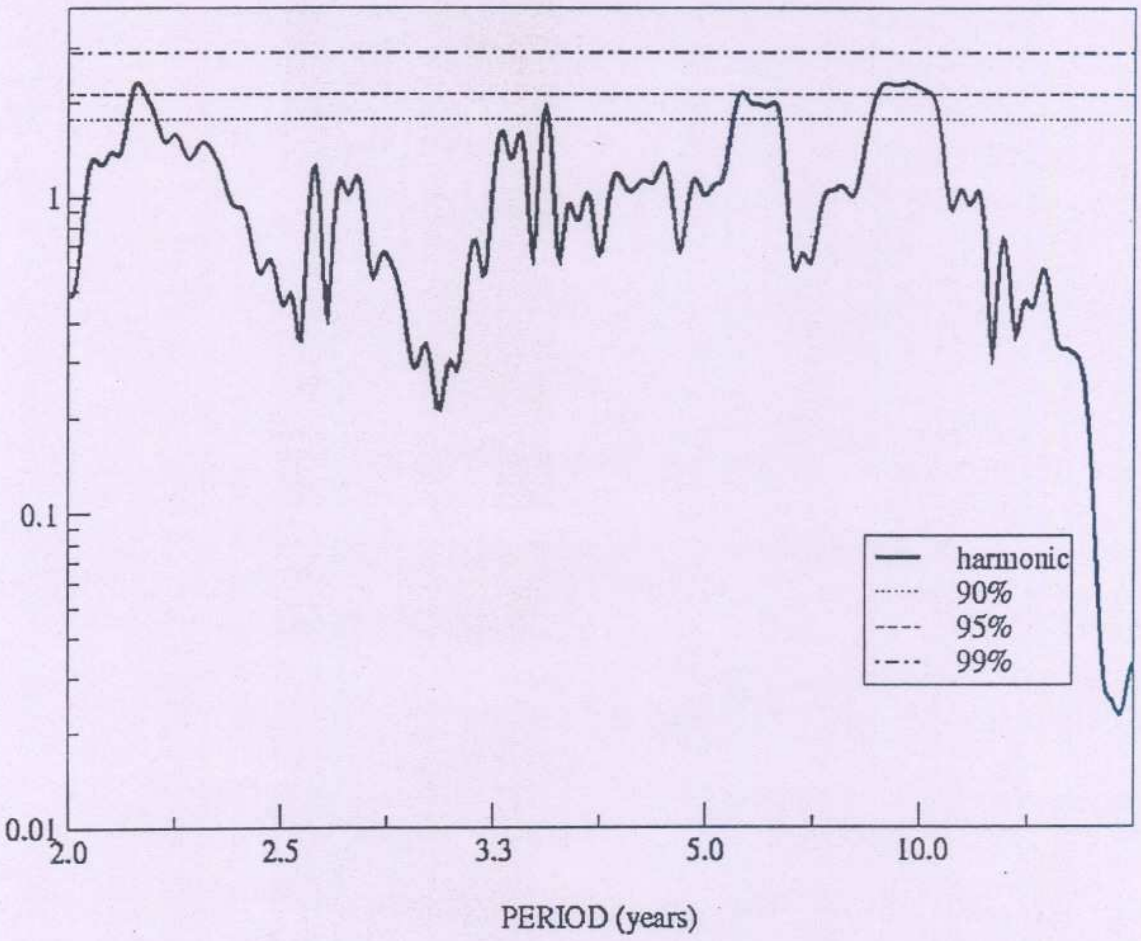

Fig. 12.— Power spectrum of time series of PC2 is shown.

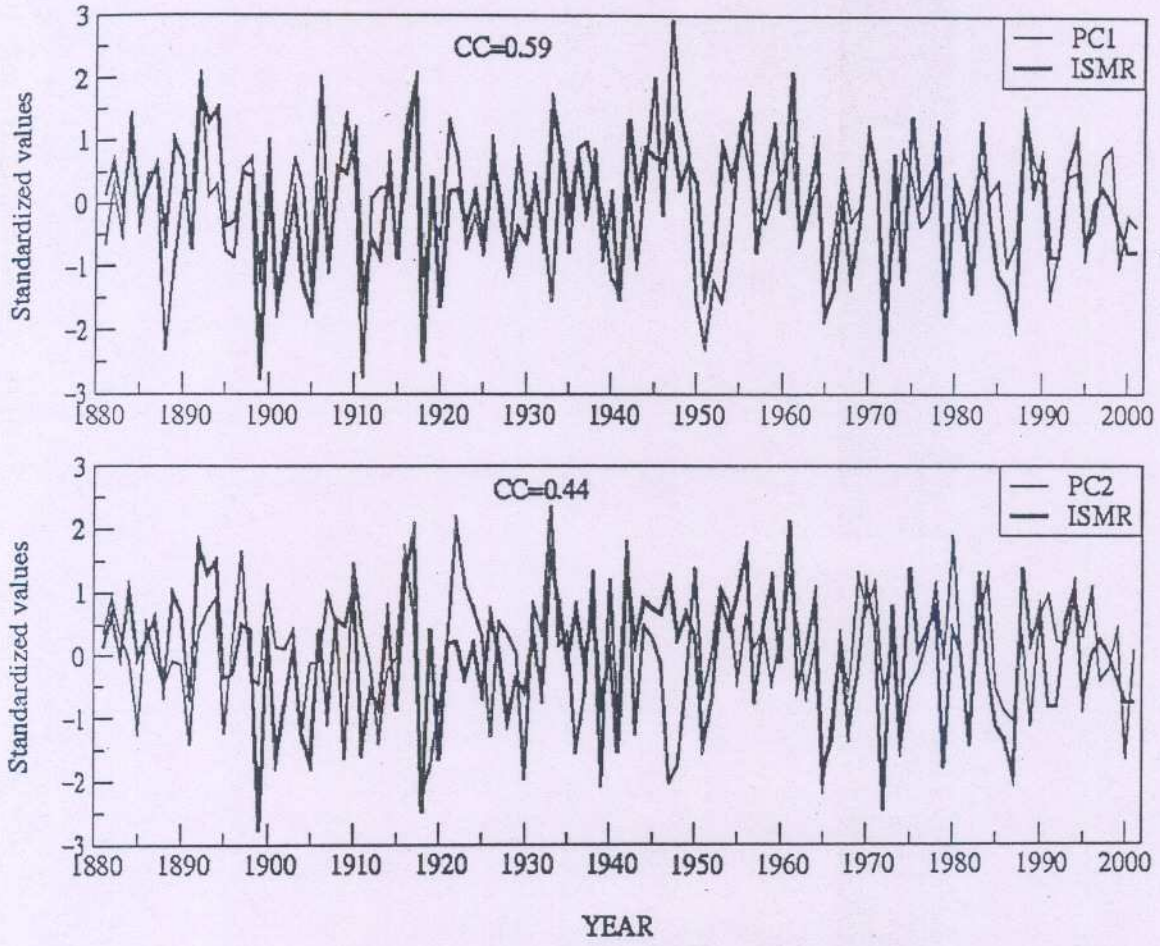

Fig. 13.— Standardized values of PC1 and PC2 time series are shown against ISMR. Also written are the values of CC in respective panels.

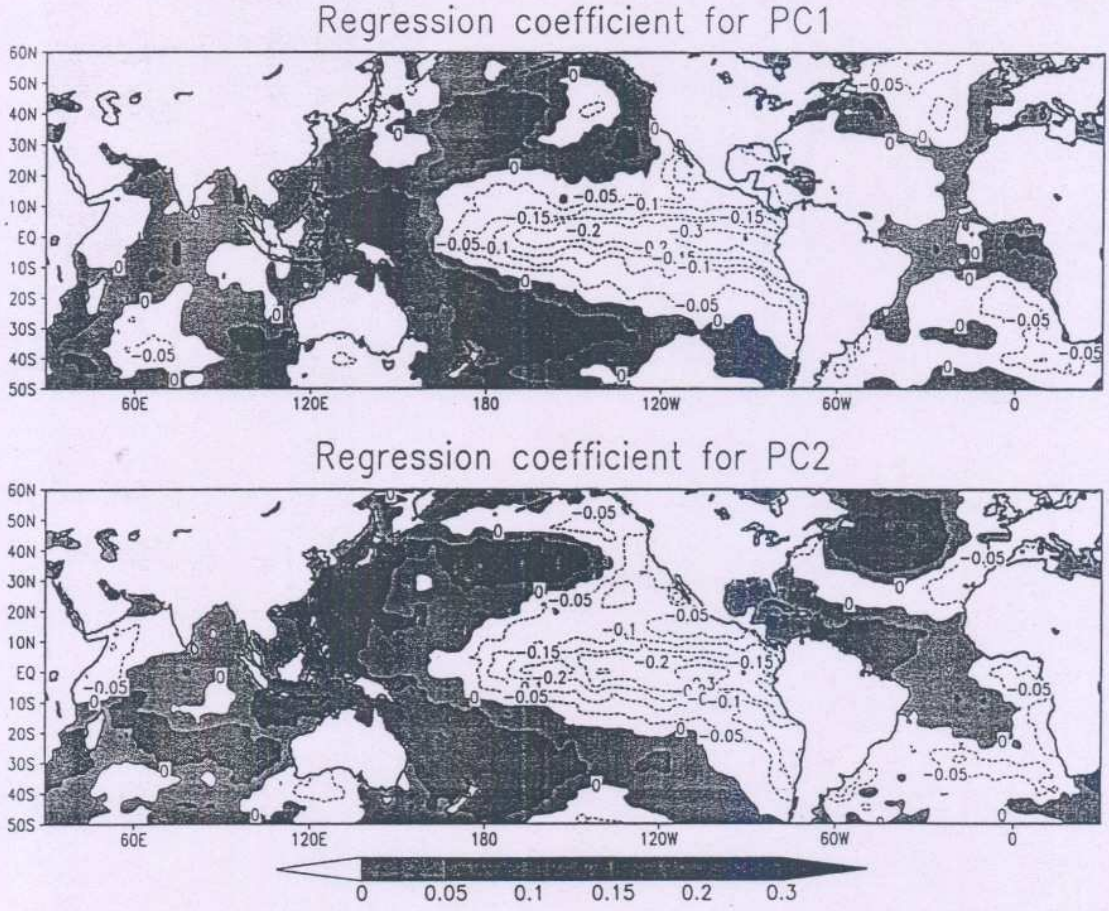

Fig. 14.— Distribution of regression coefficients for PC1 and PC2 of 18 selected regions when global JJA SST field was regressed upon PC1 and PC2. Regions with positive values are shaded.

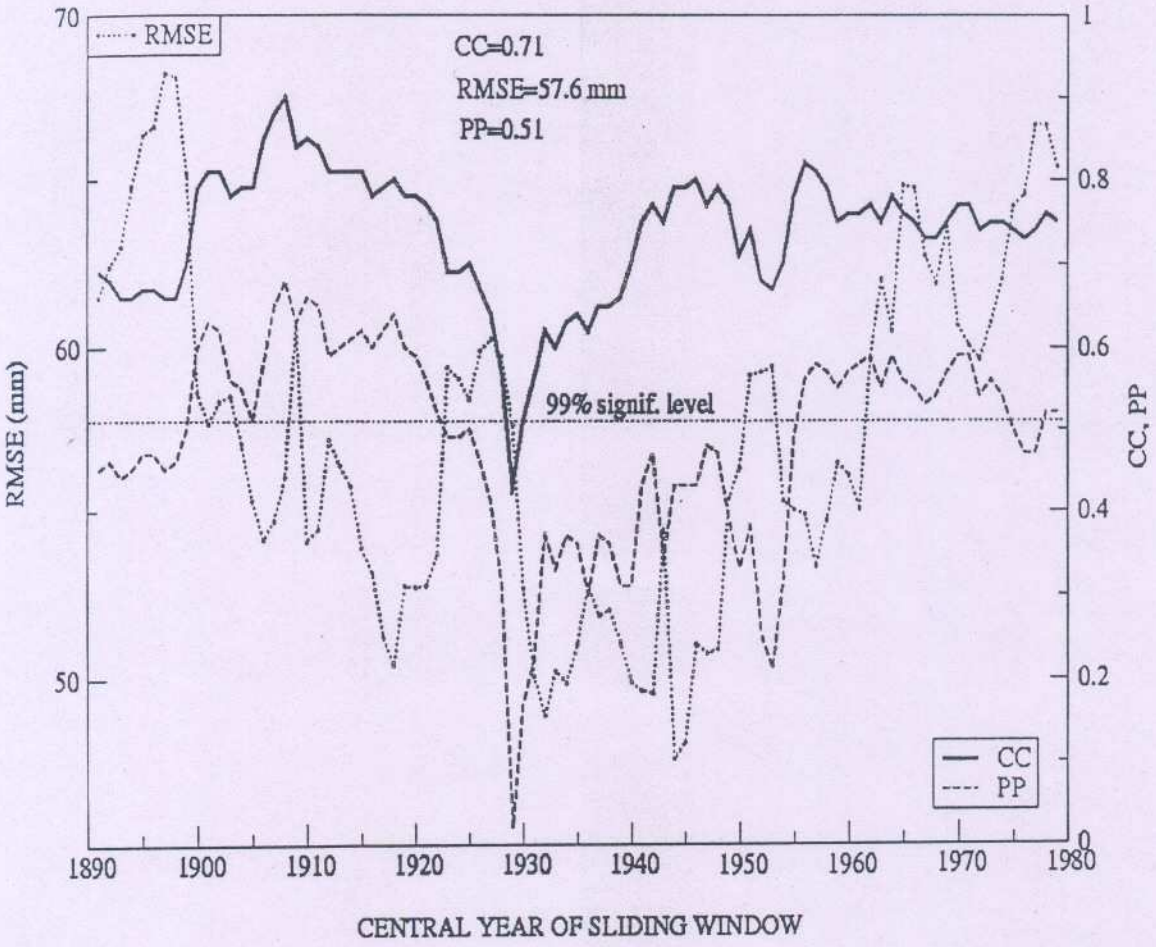

Fig. 15.— The 21- year sliding RMSE , CC and PP are shown for independent data of model development period. In this case prediction is done using PC1 and PC2 of 18 selected predictors. 99% significance level line for CC is also drawn.

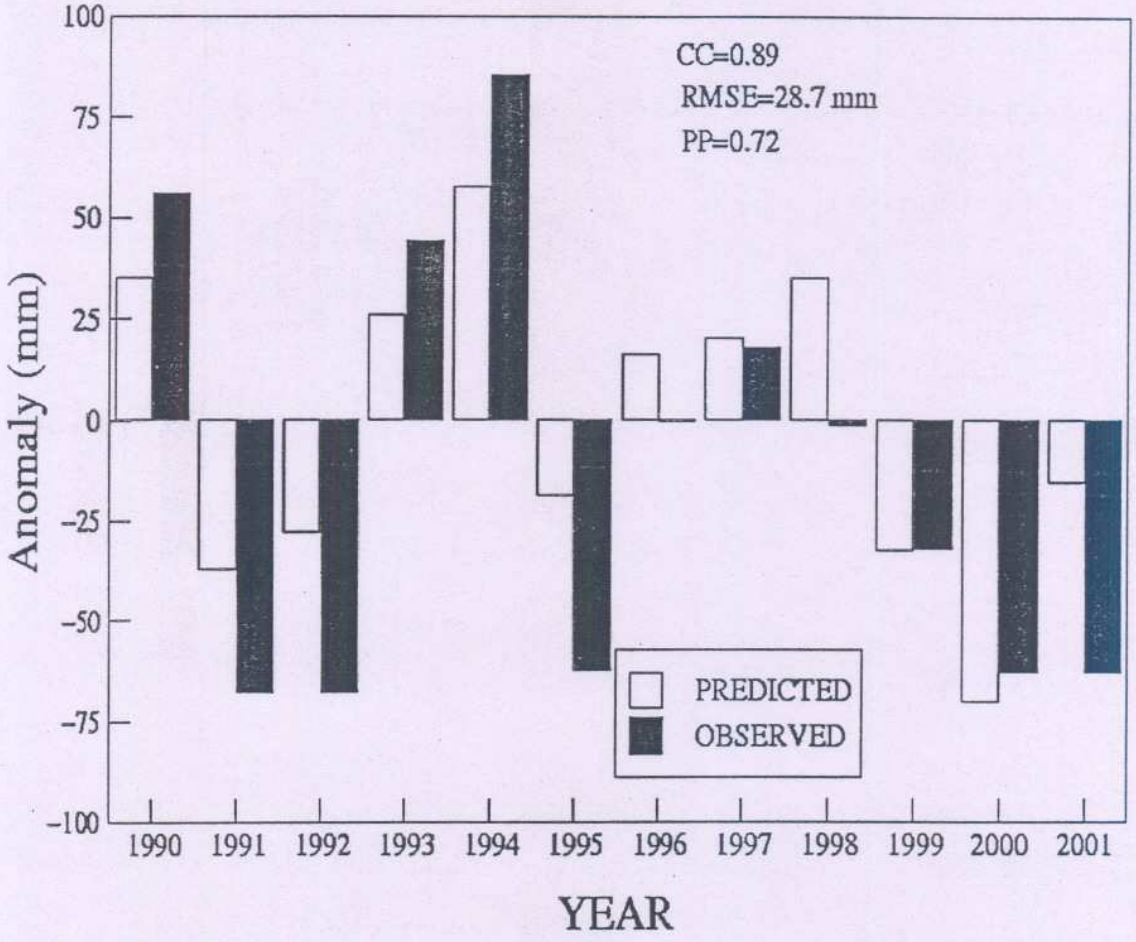

Fig. 16.— Predicted and observed ISMR anomalies for model verification period. The perdiction in this case was done using PC1 and PC2 of 18 selected predictors. Values of CC, RMSE and PP for this period are also written.

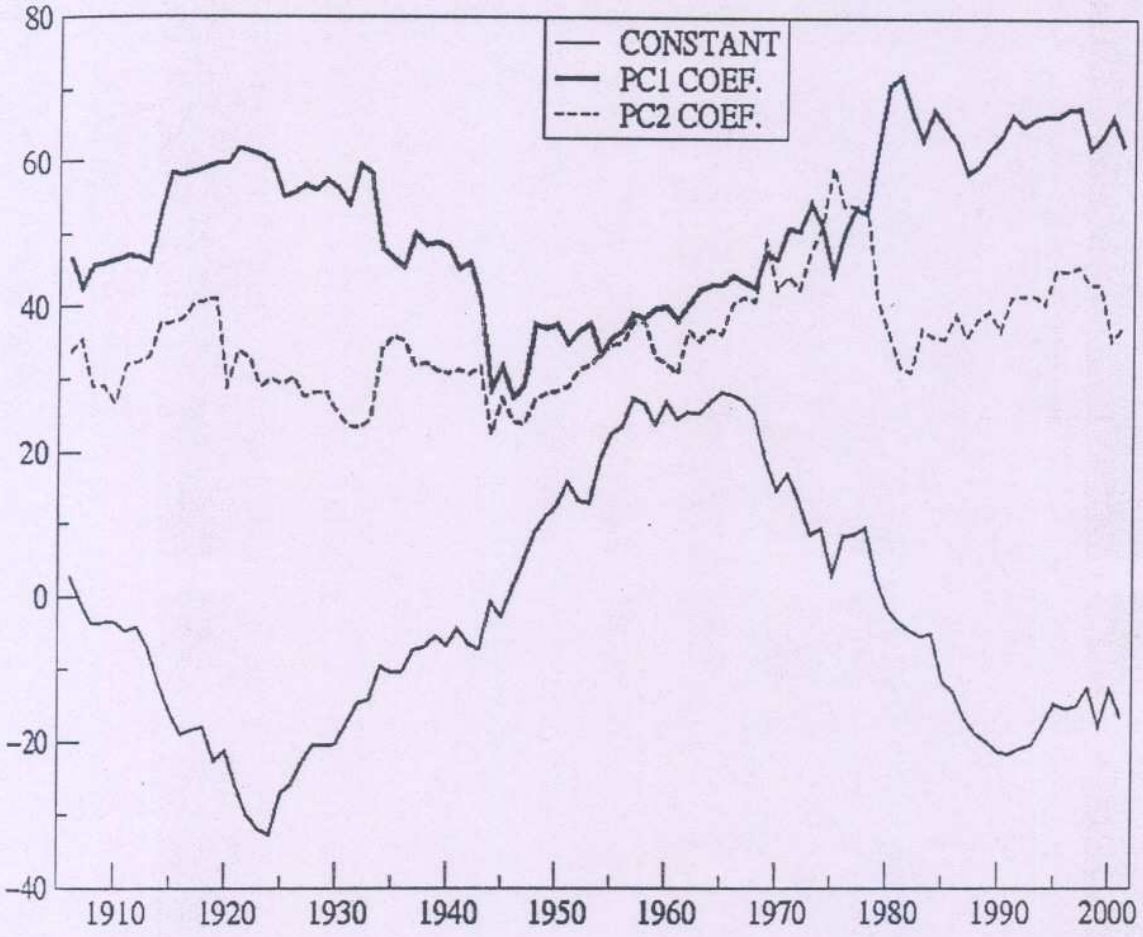

Fig. 17.— Values of constant, coefficients of PC1 and PC2 in the regression equation when regression equation was derived using previous 25 years and prediction is done one year in future (year is shown on x-axis).

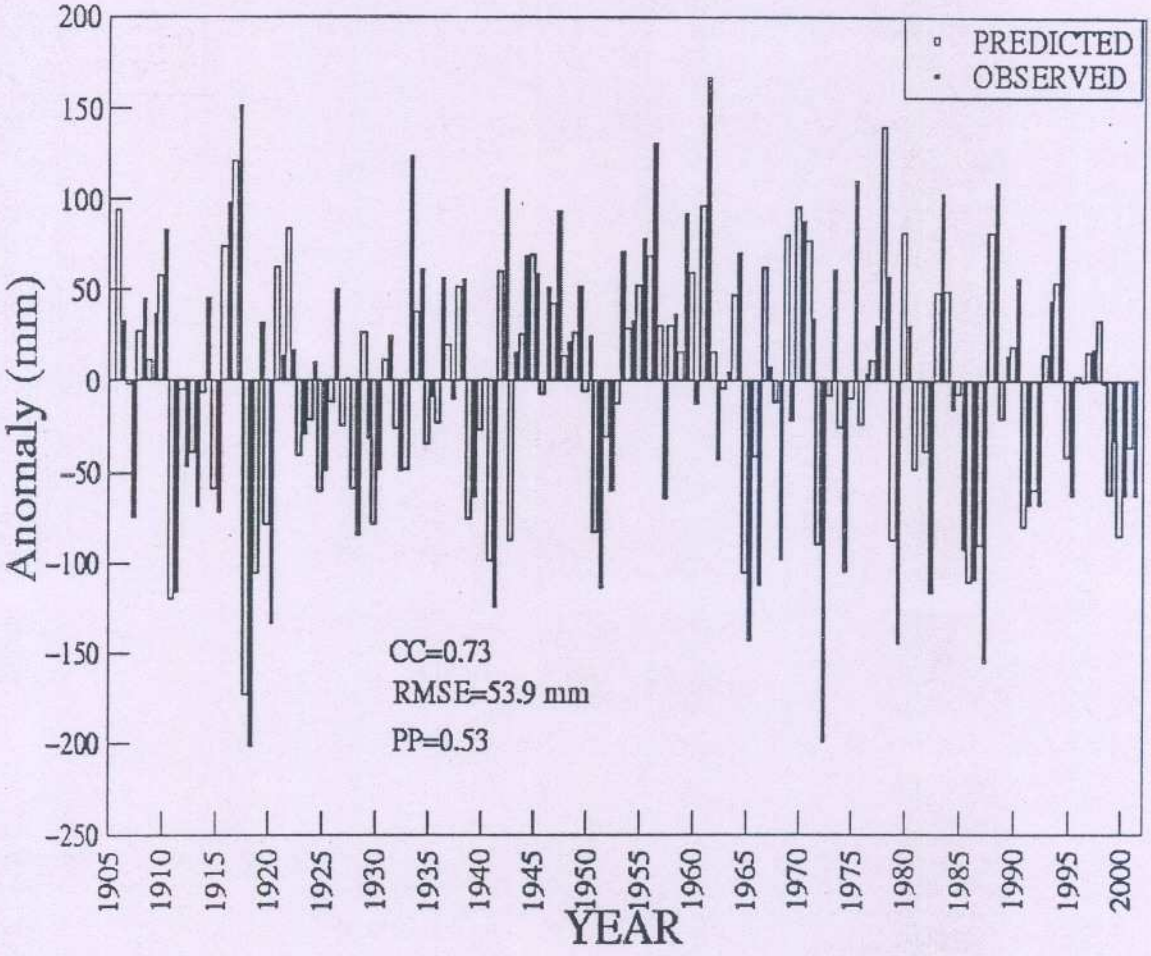

Fig. 18.— Predicted and observed ISMR anomalies for entire period (1906-2001) when regression equation was derived using previous 25 years and prediction is done one year in future. The prediction in this case was done using PC1 and PC2 of 18 selected predictors. Values of CC, RMSE and PP for this period are also written.

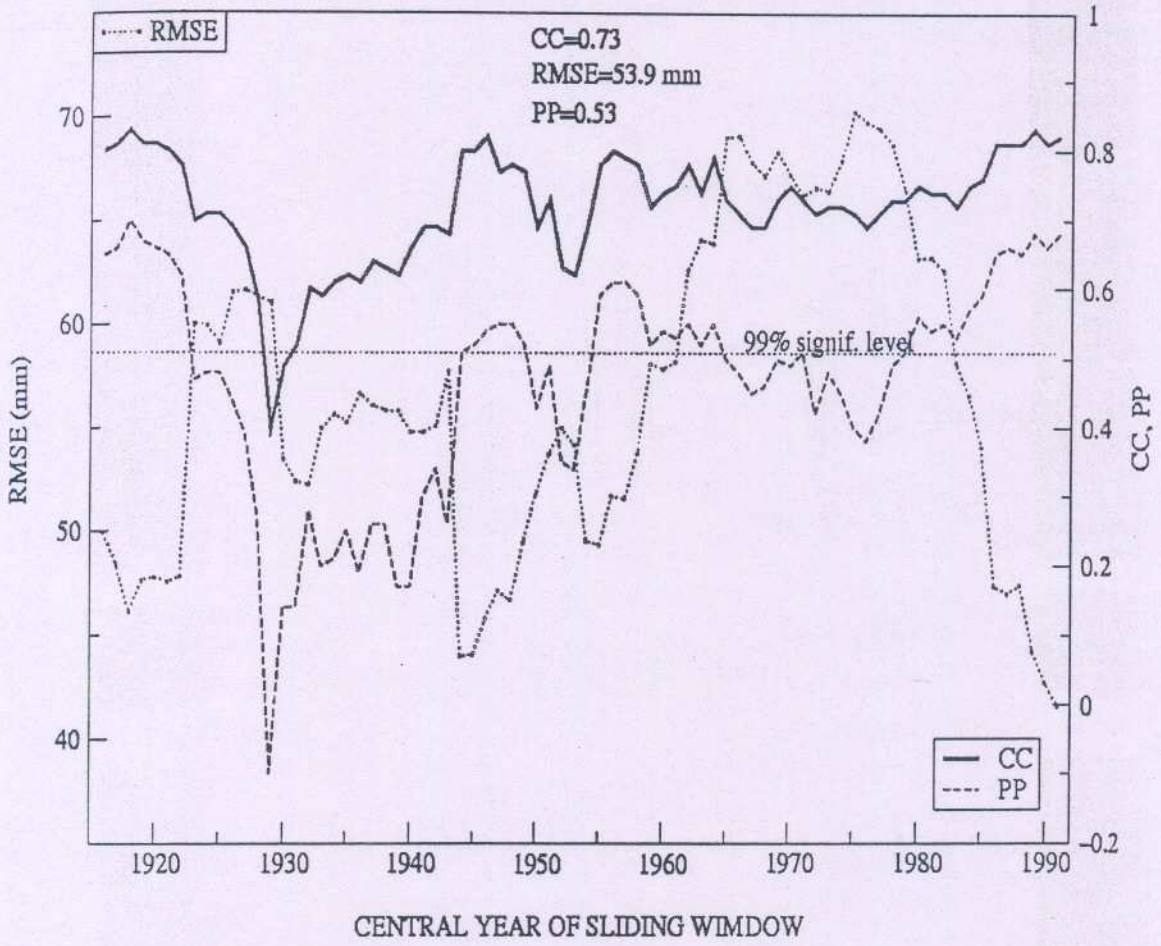

Fig. 19.— The 21- year sliding RMSE , CC and PP are shown when regression equation was derived using previous 25 years and prediction is done one year in future. In this case prediction is done using PC1 and PC2 of 18 selected predictors. 99% significance level line for CC is also drawn.

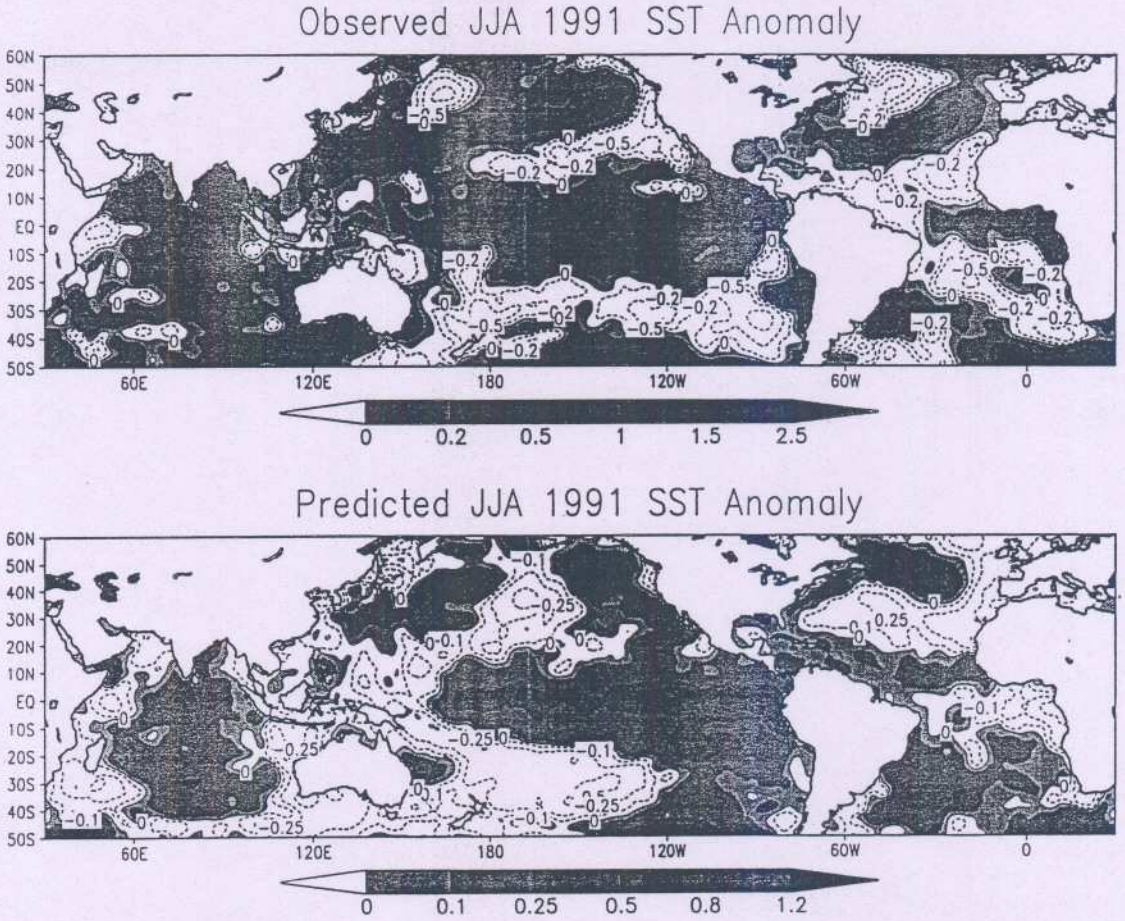

Fig. 20.— Observed JJA SST anomalies and predicted (ISMR preferred) SST anomalies for the year 1991. The prediction of SST is done using regression equation involving PC1 nad PC2 of selected 18 regions and previous 25 years SST. Regions with positive anomalies are shaded.

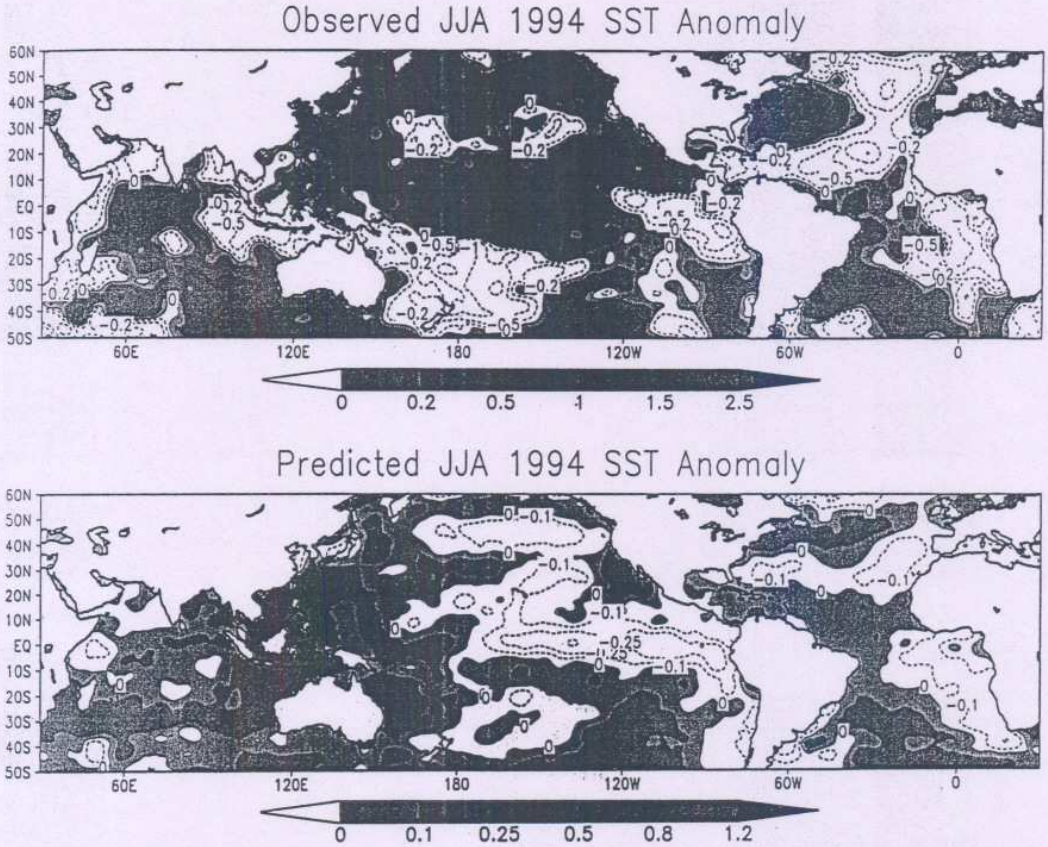

Fig. 21.— Same as Fig. 19 but for year 1994.

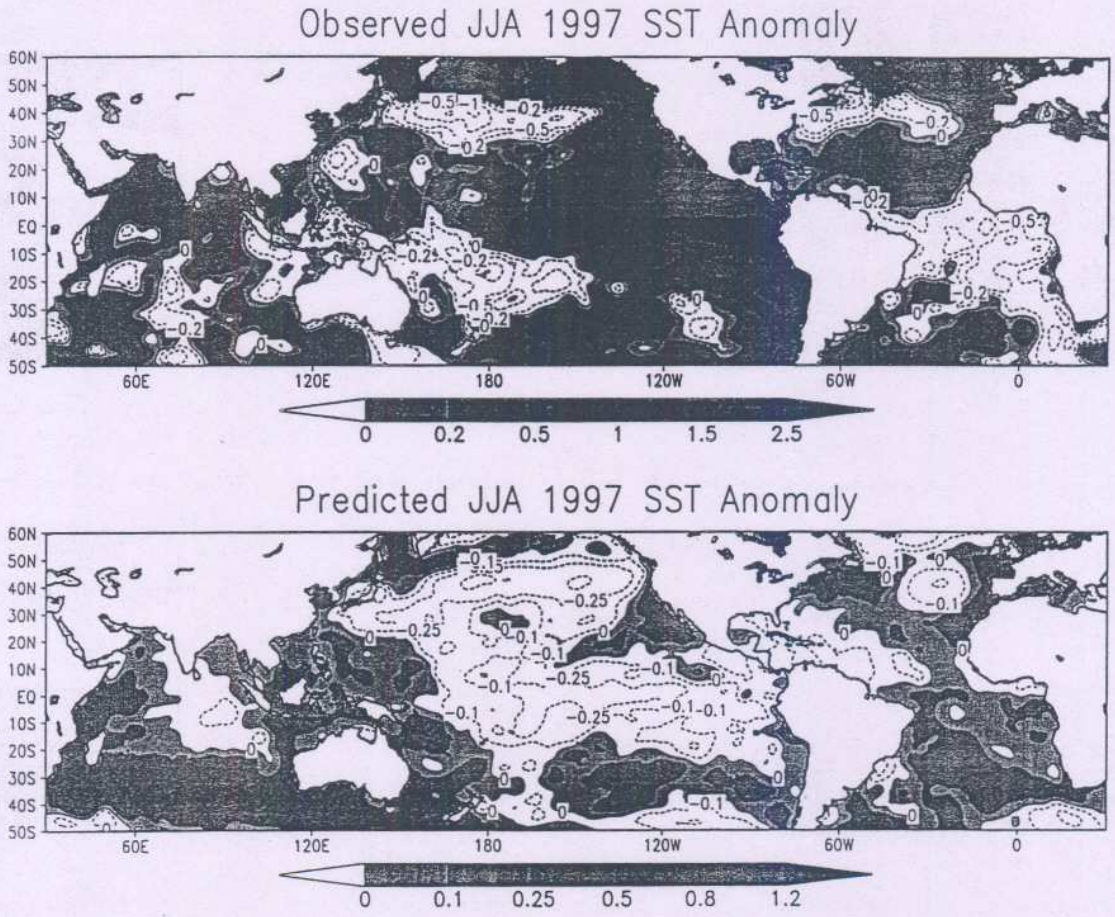

Fig. 22.— Same as Fig. 19 but for year 1997.

I. I. T. M. RESEARCH REPORTS

- Energetic consistency of truncated models, *Asnani G.C.*, August 1971, RR-001.
- Note on the turbulent fluxes of heat and moisture in the boundary layer over the Arabian Sea, *Sinha S.*, August 1971, RR-002.
- Simulation of the spectral characteristics of the lower atmosphere by a simple electrical model and using it for prediction, *Sinha S.*, September 1971, RR-003.
- Study of potential evapo-transpiration over Andhra Pradesh, *Rakhecha P.R.*, September 1971, RR-004.
- Climatic cycles in India-1: Rainfall, *Jagannathan P. and Parthasarathy B.*, November 1971, RR-005.
- Tibetan anticyclone and tropical easterly jet, *Raghavan K.*, September 1972, RR-006.
- Theoretical study of mountain waves in Assam, *De U.S.*, February 1973, RR-007.
- Local fallout of radioactive debris from nuclear explosion in a monsoon atmosphere, *Saha K.R. and Sinha S.*, December 1972, RR-008.
- Mechanism for growth of tropical disturbances, *Asnani G.C. and Keshavamurty R.N.*, April 1973, RR-009.
- Note on "Applicability of quasi-geostrophic barotropic model in the tropics", *Asnani G.C.*, February 1973, RR-010.
- On the behaviour of the 24-hour pressure tendency oscillations on the surface of the earth, Part-I: Frequency analysis, Part-II: Spectrum analysis for tropical stations, *Misra B.M.*, December 1973, RR-011.
- On the behaviour of the 24 hour pressure tendency oscillations on the surface of the earth, Part-III : Spectrum analysis for the extra-tropical stations, *Misra B.M.*, July 1976, RR-011A.
- Dynamical parameters derived from analytical functions representing Indian monsoon flow, *Awade S.T. and Asnani G.C.*, November 1973, RR-012.
- Meridional circulation in summer monsoon of Southeast Asia, *Asnani G.C.*, November 1973, RR-014.
- Energy conversions during weak monsoon, *Keshavamurty R.N. and Awade S.T.*, August 1974, RR-015.
- Vertical motion in the Indian summer monsoon, *Awade S.T. and Keshavamurty R.N.*, August 1974, RR-016.
- Semi-annual pressure oscillation from sea level to 100mb in the northern hemisphere, *Asnani G.C. and Verma R.K.*, August 1974, RR-017.
- Suitable tables for application of gamma probability model to rainfall, *Mooley D.A.*, November 1974, RR-018.

- Annual and semi-annual thickness oscillation in thenorthern hemisphere, *Asnani G.C. and Verma R.K.*, January 1975, RR-020.

- Spherical harmonic analysis of the normal constant pressure charts in the northern hemisphere, *Awade S.T., Asnani G.C. and Keshavamurty R.N.*, May 1978, RR-021.

- Dynamical parameters derived from analytical function representing normal July zonal flow along 87.5 °E, *Awade S.T. and Asnani G.C.*, May 1978, RR-022.

- Study of trends and periodicities in the seasonal and annual rainfall of India, *Parthasarathy B. and Dhar O.N.*, July 1975, RR-023.

- Southern hemisphere influence on Indian rainfall, *Raghavan K.., Paul D.K. and Upasani P.U.*, February 1976, RR-024.

- Climatic fluctuations over Indian region - Rainfall : A review, *Parthasarathy B. and Dhar O.N.*, May 1978, RR-025.

- Annual variation of meridional flux of sensible heat, *Verma R.K. and Asnani G.C.*, December 1978, RR-026.

- Poisson distribution and years of bad monsoon over India, *Mooley D.A and Parthasarathy B.*, April 1980, RR-027.

- On accelerating the FFT of Cooley and Tukey, *Mishra S.K.*, February 1981, RR-028.

- Wind tunnel for simulation studies of the atmospheric boundary layer, *Sivaramakrishnan S.*, February 1981, RR-029.

- Hundred years of Karnataka rainfall, *Parthasarathy B. and Mooley D.A.*, March 1981, RR-030.

- Study of the anomalous thermal and wind patterns during early summer season of 1979 over the Afro-Asian region in relation to the large-scale performance of the monsoon over India, *Verma R.K. and Sikka D.R.*, March 1981, RR-031.

- Some aspects of oceanic ITCZ and its disturbances during the onset and established phase of summer monsoon studied with Monex-79 data, *Sikka D.R., Paul D.K. and Singh S.V.*, March 1981, RR- 032.

- Modification of Palmer drought index, *Bhalme H.N. and Mooley D.A.*, March 1981, RR-033.

- Meteorological rocket payload for Menaka-II/Rohini 200 and its developmental details, *Vernekar K.G. and Brij Mohan*, April 1981, RR-034.

- Harmonic analysis of normal pentad rainfall of Indian stations, *Anathakrishnan R. and Pathan J.M.*, October 1981, RR-035.

- Pentad rainfall charts and space-time variations of rainfall over India and the adjoining areas, *Anathakrishnan R. and Pathan J.M.*, November 1981, RR-036.

- Dynamic effects of orography on the large scale motion of the atmosphere Part I : Zonal flow and elliptic barrier with maximum height of one km., *Bavadekar S.N. and Khaladkar R.M.*, January 1983, RR-037.

- Limited area five level primitive equation model, *Singh S.S.*, February 1983, RR-038.
- Developmental details of vortex and other aircraft thermometers, *Vernekar K.G., Brij Mohan and Srivastava S.*, November 1983, RR-039.
- Note on the preliminary results of integration of a five level P.E. model with westerly wind and low orography, *Bavadekar S.N., Khaladkar R.M., Bandyopadhyay A. and Seetaramayya P.*, November 1983, RR-040.
- Long-term variability of summer monsoon and climatic change, *Verma R.K., Subramaniam K. and Dugam S.S.*, December 1984, RR-041.
- Project report on multidimensional initialization for NWP models, *Sinha S.*, February 1989, RR-042.
- Numerical experiments with inclusion of orography in five level P.E. Model in pressure-coordinates for interhemispheric region, *Bavadekar S.N. and Khaladkar R.M.*, March 1989, RR-043.
- Application of a quasi-lagrangian regional model for monsoon prediction, *Singh S.S. and Bandyopadhyay A.*, July 1990, RR-044.
- High resolution UV-visible spectrometer for atmospheric studies, *Bose S., Trimbake H.N., Londhe A.L. and Jadhav D.B.*, January 1991, RR-045.
- Fortran-77algorithm for cubic spline interpolation for regular and irregular grids, *Tandon M.K.*, November 1991, RR-046.
- Fortran algorithm for 2-dimensional harmonic analysis, *Tandon M.K.*, November 1991, RR- 047.
- 500 hPa ridge and Indian summer monsoon rainfall : A detailed diagnostic study, *Krishna Kumar K., Rupa Kumar K. and Pant G.B.*, November 1991, RR-048.
- Documentation of the regional six level primitive equation model, *Singh S.S. and Vaidya S.S.*, February 1992, RR-049.
- Utilisation of magnetic tapes on ND-560 computer system, *Kripalani R.H. and Athale S.U.*, July 1992, RR-050.
- Spatial patterns of Indian summer monsoon rainfall for the period 1871-1990, *Kripalani R.H., Kulkarni A.A., Panchawagh N.V. and Singh S.V.*, August 1992, RR-051.
- FORTRAN algorithm for divergent and rotational wind fields, *Tandon M.K.*, November 1992, RR-052.
- Construction and analysis of all-India summer monsoon rainfall series for the longest instrumental period: 1813-1991, *Sontakke N.A., Pant G.B. and Singh N.*, October 1992, RR-053.
- Some aspects of solar radiation, *Tandon M.K.*, February 1993, RR-054.
- Design of a stepper motor driver circuit for use in the moving platform, *Dharmaraj T. and Vernekar K.G.*, July 1993, RR-055.

- Experimental set-up to estimate the heat budget near the land surface interface, *Vernekar K.G., Saxena S., Pillai J.S., Murthy B.S., Dharmaraj T. and Brij Mohan*, July 1993, RR-056.

- Identification of self-organized criticality in atmospheric total ozone variability, *Selvam A.M. and Radhamani M.*, July 1993, RR-057.

- Deterministic chaos and numerical weather prediction, *Selvam A.M.*, February 1994, RR-058.

- Evaluation of a limited area model forecasts, *Singh S.S., Vaidya S.S Bandyopadhyay A., Kulkarni A.A, Bawiskar S.M.,Sanjay J., Trivedi D.K. and Iyer U.*, October 1994, RR-059.

- Signatures of a universal spectrum for atmospheric interannual variability in COADS temperature time series, *Selvam A.M., Joshi R.R. and Vijayakumar R.*, October 1994, RR-060.

- Identification of self-organized criticality in the interannual veriability of global surface temperature, *Selvam A.M. and Radhamani M.*, October 1994, RR-061.

- Identification of a universal spectrum for nonlinear veriability of solar-geophysical parameters, *Selvam A.M., Kulkarni M.K., Pethkar J.S. and Vijayakumar R.*, October 1994, RR-062.

- Universal spectrum for fluxes of energetic charged particles from the earth's magnetosphere, *Selvam A.M. and Radhamani M.*, June 1995, RR-063.

- Estimation of nonlinear kinetic energy exchanges into individual triad interactions in the frequency domain by use of the cross-spectral technique, *Chakraborty D.R.*, August 1995, RR-064.

- Monthly and seasonal rainfall series for all-India homogeneous regions and meteorological subdivisions: 1871-1994, *Parthasarathy B., Munot A.A. and Kothawale D.R.*, August 1995, RR-065.

- Thermodynamics of the mixing processes in the atmospheric boundary layer over Pune during summer monsoon season, *Morwal S.B. and Parasnis S.S.*, March 1996, RR-066.

- Instrumental period rainfall series of the Indian region: A documentation, *Singh N. and Sontakke N.A.*, March 1996, RR-067.

- Some numerical experiments on roundoff-error growth in finite precision numerical computation, *Fadnavis S.*, May 1996, RR-068.

- Fractal nature of MONTBLEX time series data, *Selvam A.M. and Sapre V.V.*, May 1996, RR-069.

- Homogeneous regional summer monsoon rainfall over India: Interannual variability and teleconnections, *Parthasarathy B., Rupa Kumar K. and Munot A.A.*, May 1996, RR-070.

- Universal spectrum for sunspot number variability, *Selvam A.M. and Radhamani M.*, November 1996, RR-071.

- Development of simple reduced gravity ocean model for the study of upper north Indian ocean, *Behera S.K. and Salvekar P.S.*, November 1996, RR-072.

- Study of circadian rhythm and meteorological factors influencing acute myocardial infraction, *Selvam A.M., Sen D. and Mody S.M.S.*, April 1997, RR-073.

- Signatures of universal spectrum for atmospheric gravity waves in southern oscillation index time series, *Selvam A.M., Kulkarni M.K., Pethkar J.S. and Vijayakumar R.*, December 1997, RR-074.

- Some example of X-Y plots on Silicon Graphics, *Selvam A.M., Fadnavis S. and Gharge S.P.*, May 1998, RR-075.

- Simulation of monsoon transient disturbances in a GCM, *Ashok K., Soman M.K. and Satyan V.*, August 1998, RR-076.

- Universal spectrum for intraseasonal variability in TOGA temperature time series, *Selvam A.M., Radhamani M., Fadnavis S. and Tinmaker M.I.R.*, August 1998, RR-077.

- One dimensional model of atmospheric boundary layer, *Parasnis S.S., Kulkarni M.K., Arulraj S. and Vernekar K.G.*, February 1999, RR-078.

- Diagnostic model of the surface boundary layer - A new approach, *Sinha S.*, February 1999, RR-079.

- Computation of thermal properties of surface soil from energy balance equation using force - restore method, *Sinha S.*, February 1999, RR-080.

- Fractal nature of TOGA temperature time series, *Selvam A.M. and Sapre V.V.*, February 1999, RR-081.

- Evolution of convective boundary layer over the Deccan Plateau during summer monsoon, *Parasnis S.S.*, February 1999, RR-082.

- Self-organized criticality in daily incidence of acute myocardial infarction, *Selvam A.M., Sen D., and Mody S.M.S.*, Feburary 1999, RR-083.

- Monsoon simulation of 1991 and 1994 by GCM : Sensitivity to SST distribution, *Ashrit R.G., Mandke S.K. and Soman M.K.*, March 1999, RR-084.

- Numerical investigation on wind induced interannual variability of the north Indian Ocean SST, *Behera S.K., Salvekar P.S. and Ganer D.W.*, April 1999, RR-085.

- On step mountain eta model, *Mukhopadhyay P., Vaidya S.S., Sanjay J. and Singh S.S.*, October 1999, RR-086.

- Land surface processes experiment in the Sabarmati river basin: an overview and early results, *Vernekar K.G., Sinha S., Sadani L.K., Sivaramakrishnan S., Parasnis S.S., Brij Mohan, Saxena S., Dharamraj T., Pillai, J.S., Murthy B.S., Debaje, S.B., Patil, M.N. and Singh A.B.*, November 1999, RR-087.

- Reduction of AGCM systematic error by Artificial Neural Network: A new approach for dynamical seasonal prediction of Indian summer monsoon rainfall, *Sahai A.K. and Satyan V.*, December 2000, RR-088.

- Ensemble GCM simulations of the contrasting Indian summer monsoons of the 1987 and 1988, *Mujumdar M. and Krishnan R.*, February 2001, RR-089.

- Aerosol measurements using lidar and radiometers at Pune during INDOEX field phases, Maheskumar R.S., Devara P.C.S., Raj P.E., Jaya Rao Y.,Pandithurai G., Dani K.K., Saha S.K., Sonbawne S.M. and Tiwari Y.K., December 2001, RR-090.

- Modelling studies of the 2000 Indian summer monsoon and extended analysis, Krishnan R., Mujumdar M., Vaidya V., Ramesh K.V. and Satyan V., December 2001, RR-091.

- Intercomparison of Asian summer monsoon 1997 simulated by atmospheric general circulation models, Mandke S.K., Ramesh K.V. and Satyan V., December 2001, RR-092.